


RESEARCH

Open Access



# Targeting GPR65 alleviates hepatic inflammation and fibrosis by suppressing the JNK and NF- $\kappa$ B pathways

Kun Zhang<sup>1†</sup>, Meng-Xia Zhang<sup>1†</sup>, Xiao-Xiang Meng<sup>1†</sup>, Jing Zhu<sup>1</sup>, Jia-Jun Wang<sup>1</sup>, Yi-Fan He<sup>1</sup>, Ye-Hua Li<sup>1</sup>, Si-Cong Zhao<sup>1</sup>, Zhe-Min Shi<sup>1</sup>, Li-Na Zheng<sup>1</sup>, Tao Han<sup>2\*</sup> and Wei Hong<sup>1\*</sup> 

## Abstract

**Background** G-protein coupled receptors (GPCRs) are recognized as attractive targets for drug therapy. However, it remains poorly understood how GPCRs, except for a few chemokine receptors, regulate the progression of liver fibrosis. Here, we aimed to reveal the role of GPR65, a proton-sensing receptor, in liver fibrosis and to elucidate the underlying mechanism.

**Methods** The expression level of GPR65 was evaluated in both human and mouse fibrotic livers. Furthermore, *Gpr65*-deficient mice were treated with either bile duct ligation (BDL) for 21 d or carbon tetrachloride (CCl<sub>4</sub>) for 8 weeks to investigate the role of GPR65 in liver fibrosis. A combination of experimental approaches, including Western blotting, quantitative real-time reverse transcription-polymerase chain reaction (qRT-PCR), and enzyme-linked immunosorbent assay (ELISA), confocal microscopy and rescue studies, were used to explore the underlying mechanisms of GPR65's action in liver fibrosis. Additionally, the therapeutic potential of GPR65 inhibitor in the development of liver fibrosis was investigated.

**Results** We found that hepatic macrophages (HMs)-enriched GPR65 was upregulated in both human and mouse fibrotic livers. Moreover, knockout of *Gpr65* significantly alleviated BDL- and CCl<sub>4</sub>-induced liver inflammation, injury and fibrosis in vivo, and mouse bone marrow transplantation (BMT) experiments further demonstrated that the protective effect of *Gpr65* knockout is primarily mediated by bone marrow-derived macrophages (BMMs). Additionally, in vitro data demonstrated that *Gpr65* silencing and GPR65 antagonist inhibited, while GPR65 overexpression and application of GPR65 endogenous and exogenous agonists enhanced the expression and release of tumor necrosis factor- $\alpha$  (TNF- $\alpha$ ), interleukin-6 (IL-6) and transforming growth factor- $\beta$  (TGF- $\beta$ ), all of which subsequently promoted the activation of hepatic stellate cells (HSCs) and the damage of hepatocytes (HCs). Mechanistically, GPR65 overexpression, the acidic pH and GPR65 exogenous agonist induced up-regulation of TNF- $\alpha$  and IL-6 via the G $\alpha$ q-Ca<sup>2+</sup>-JNK/NF- $\kappa$ B pathways, while promoted the expression of TGF- $\beta$  through the G $\alpha$ q-Ca<sup>2+</sup>-MLK3-MKK7-JNK pathway. Notably, pharmacological GPR65 inhibition retarded the development of inflammation, HCs injury and fibrosis in vivo.

<sup>†</sup>Kun Zhang, Meng-Xia Zhang and Xiao-Xiang Meng contributed equally to this work.

\*Correspondence:

Tao Han

hantaomd@126.com

Wei Hong

hongwei@tmu.edu.cn

Full list of author information is available at the end of the article



**Conclusions** GPR65 is a major regulator that modulates the progression of liver fibrosis. Thus, targeting GPR65 could be an effective therapeutic strategy for the prevention of liver fibrosis.

**Keywords** GPR65, Hepatic fibrosis, Hepatic macrophages, Inflammation, JNK, NF- $\kappa$ B

## Background

Hepatic fibrosis has emerged as a major chronic liver pathological process, characterized by the excessive deposition of extracellular matrix (ECM), the development of inflammation and hepatic injury [1]. This process is caused by a persistent hepatic damage and injury repair response induced by various etiologies including biliary obstruction, hepatitis B/C virus infection and alcohol abuse [1–3]. If the damage persists, the fibrotic process will result in liver failure and cirrhosis, causing more than 1.32 million deaths annually globally [4]. Regrettably, no effective drug for the treatment of hepatic fibrosis has been approved by the Food and Drug Administration so far. Therefore, a more detailed understanding of the pathophysiological mechanism of fibrosis is needed to develop promising drug targets and corresponding therapeutic molecules that prevent the progression of hepatic fibrosis.

G-protein coupled receptors (GPCRs), which are the largest superfamily of transmembrane proteins encoded by the human genome, mediate the majority of cellular responses to external stimuli, including light, odors, ions, hormones, and growth factors [5, 6]. Although GPCRs as the most productive drug targets, are targeted by one-third of the drugs in clinical use, few GPCRs are reported to be involved in hepatic fibrosis except for a few chemokine receptors [6, 7]. GPR65 (also known as TDAG8) was initially identified as orphaned GPCR in apoptotic thymocytes [8]. Currently, it has been accepted that GPR65, along with GPR4, GPR68 (also known as OGR1) and GPR132 (also known as G2A), forms a group of proton-sensing GPCRs [9]. The signaling networks downstream of GPR65 have been implicated in many pathophysiological processes including tumor, immune-related diseases and inflammation through *Gas*/cyclic AMP/protein kinase A/cAMP-responsive-element-binding protein (*Gas*/cAMP/PKA/CREB) and *Gaq*/phospholipase C beta/protein kinase C (*Gaq*/PLC- $\beta$ /PKC) pathways in response to extracellular stimuli [10–12]. However, GPR65 may have both protective and detrimental roles [10, 11, 13–15], for example, it is downregulated in hematological malignancies and functions as a tumor suppressor to promote apoptosis of murine lymphoma cells [10]. Also, GPR65 partly mediates the inhibition of extracellular acidification-induced pro-inflammatory cytokines via the *Gas*/PKA pathway [11]. On the other hand, GPR65 functions as an oncogenic GPCR as it is increased in a

series of human cancer tissues [13]. Similarly, blocking GPR65 expression and function is associated with reduced pro-inflammatory cytokines releasing, microglial activation and eosinophil viability [12, 14]. Hepatic macrophages (HMs) are heterogeneous cell populations, consisting of liver-resident macrophages, traditionally termed Kupffer cells (KCs), and monocyte-derived macrophages that are recruited from the circulation upon acute or chronic liver injury [16, 17]. Additionally, macrophages can be broadly classified into two main subsets: classically activated macrophages (M1), characterized by a pro-inflammatory phenotype, and alternatively activated macrophages (M2), which are associated with anti-inflammatory and tissue repair functions [16, 17]. Nevertheless, the function of GPR65 in HMs in the process of inflammation and fibrosis is still unclear.

In the present study, we identified that HMs-enriched GPR65 was increased in both human and mouse fibrotic livers and HMs from fibrotic livers. We conducted a series of experiments, such as gain- and loss-of-function assays, the application of the specific antagonist and agonist of GPR65, and combined with *Gpr65*-deficient mice as well as mouse bone marrow transplantation (BMT) experiments to investigate the function and the underlying mechanisms of GPR65 in HMs, hepatic stellate cells (HSCs) and hepatocytes (HCs), and the intercellular network during liver fibrogenesis, thus providing a new therapeutic strategy for the prevention of liver fibrosis.

## Methods

### Animals in vivo study

All of the animal works were conducted according to the approved guidelines and approved by the Animal Care and Use Committee of Tianjin Medical University (TMUaMEC2018025). Male 6–8 weeks wild-type (WT) mice and *Gpr65* knockout (GPR65-KO) mice, which were generated using CRISPR-Cas9 technology (Cyagen Biosciences, Suzhou, China) on a C57BL/6N background were used in the carbon tetrachloride (CCl<sub>4</sub>)- or bile duct ligation (BDL)-induced hepatic fibrosis models, as previously described [18, 19]. In brief, the gRNAs sequences targeting *Gpr65* were gRNA1: GGAGATTGGTCCGGTGCAAATGGG; gRNA2: ATAACCCCTAAGAAGCACGCGGG. The primers used for identification were as follows: upstream primer 1: 5'-AATGTGACTTTTGGAAATGCC-3'; upstream primer 2: 5'-ATAGACTAAGAG

GTGGAGGC-3'; downstream primer: 5'-AACTAG GCAGGGTCAATTCC-3'. Sequence primer for the product: 5'-AATGTGACTTTTGAAATGCC-3'. WT and GPR65-KO mice came from the same heterozygous mice and hosted under pathogen-free conditions. WT or GPR65-KO mice were separated into 2 groups randomly: WT ( $n=5$ ) and WT + CCl<sub>4</sub>/BDL ( $n=10$ ) or GPR65-KO ( $n=5$ ) and GPR65-KO + CCl<sub>4</sub>/BDL ( $n=10$ ). Thirty 6–8 weeks-old BALB/c male mice were purchased from Beijing HFK Bioscience (Beijing, China) and separated into 4 groups randomly: Ctrl ( $n=5$ ), Ctrl + CCl<sub>4</sub> ( $n=10$ ), ZINC62678696 (the inhibitor of GPR65;  $n=5$ ), ZINC62678696 + CCl<sub>4</sub> ( $n=10$ ). The GPR65 inhibitor (10 mg/kg) was administered 4 weeks after the first CCl<sub>4</sub> injection every two days. For CCl<sub>4</sub>-induced hepatic fibrosis mouse model, mice were treated with 0.25 ml/kg CCl<sub>4</sub> dissolved in olive oil or olive oil twice a week via intraperitoneal injection for 6–8 weeks. For BDL-induced hepatic fibrosis mouse model, mice were administered BDL operation or sham operation and were sacrificed under anesthesia with 3% sodium pentobarbital (45 mg/kg, ip) after 21 d. For mouse BMT experiments, the male WT recipient mice at 8 weeks of age were given lethal irradiation with 9 Gy (RS2000PRO-225 X-RAY, 4.5 Gy twice between 4 h) and then intravenous injection of  $1 \times 10^7$  bone marrow cells (100–150  $\mu$ l) harvested from WT or GPR65-KO donor mice ( $n=8$ ). Four weeks after irradiation and BMT, the chimeric mice were treated with 0.25 ml/kg CCl<sub>4</sub> dissolved in olive oil thrice a week via intraperitoneal injection for 6 weeks. Serums and liver specimens were collected for further analyses.

#### Patient samples

Six normal livers and 28 human fibrotic livers were obtained from Tianjin Third Central Hospital (Tianjin, China) as previously reported [18, 20, 21]. All subjects were of the same ethnicity. Clinical and pathological characteristics including age, gender, alanine aminotransferase (ALT), aspartate aminotransferase (AST),  $\gamma$ -glutamyl transpeptidase (GGT) and etiologies were recorded and summarized in Additional file 1: Table S1. For histological scoring of liver fibrosis, we stained paraffin-embedded 5  $\mu$ m liver sections with Sirius red staining, HE staining and Masson's trichrome staining. Hepatic fibrosis was scored (stages F0–F4) according to the METAVIR fibrosis stage system by three hepatopathologists blinded to the study protocol and stratified as normal liver (F0), mild fibrosis (F1–F2) or advanced fibrosis (F3–F4). The research methods were consistent with the standards in the Helsinki Declaration. Written informed consents were acquired from each patient and the study has been approved by the local Ethical Committee of Tianjin Third Central Hospital (SZX-IRB2020-005-02).

#### Culture and treatments of primary cells and cell lines

Mouse primary HMs, HSCs, HCs and liver sinusoidal endothelial cells (LSECs) were isolated by in situ perfusion digestion as previously reported [17–21]. HMs, HCs, and LSECs were isolated from 8 to 10 weeks-old male mice, while HSCs was isolated from male BALB/c mice at 40 weeks of age. In brief, mice were anaesthetized via sodium pentobarbital (3%, ip). Sequential infusion of ethylene glycol bis(2-aminoethyl ether) tetraacetic acid (EGTA, 2 min), 0.05% pronase E (10 min, Roche, Germany, Cat# 11459643001), 0.025% collagenase type IV (10 min, Sigma-Aldrich, USA, Cat# C5138) were performed via the portal vein. Liver tissues were then digested in GBSS/B containing 0.033% pronase E (Roche, Germany, Cat# 11459643001), 0.04% collagenase type IV (Sigma-Aldrich, USA, Cat# C5138) and 1% DNase 1 (Roche, Germany, Cat# 10104159001) for 20 min at 37 °C in shaker bath. The digested cell suspension was then filtered via a 70 mm cell filter and centrifuged at 50 g for 6 min three times to remove HCs. HMs, HSCs and LSECs were isolated from the suspension using 8.2%, 12% and 18% Histodenz solution (Sigma-Aldrich, USA, Cat# D2158) at 1450 g for 22 min. Selective adhesion or magnetic-activated cell sorting (MACS)-based positive selection using an F4/80 antibody (Miltenyi Biotec, Germany, Cat# 130-110-443) and a CD146 antibody (Miltenyi Biotec, Germany, Cat# 130-092-007) were used to purify HMs and LSECs respectively. The purity of HSCs was detected by perinuclear lipid droplets and morphology when the primary HSCs were isolated, and we performed  $\alpha$ -smooth muscle actin ( $\alpha$ -SMA) staining in primary HSCs at day 7. Trypan blue exclusion assay was used to measure the cell viability. All primary cells were maintained in Dulbecco's Modified Eagle's Medium (DMEM, Gibco, USA, Cat# C11995500BT) containing 10% fetal bovine serum (FBS, Gibco, USA, Cat# 16000-044), and 1% penicillin/streptomycin (Solarbio, China, Cat# P1400). In addition, primary HCs and LSECs were seeded in plates coated with type I collagen (Sigma-Aldrich, USA, Cat# C7661).

The murine immortalized macrophages RAW264.7, human umbilical vein endothelial cells (HUVECs) and HEK-293T cells (ATCC, USA) were cultured in DMEM containing 10% FBS, 1% penicillin/streptomycin (Solarbio, China, Cat# P1400). Human hepatic stellate cell line LX-2 cells (Sigma-Aldrich, USA) were maintained in DMEM (Gibco, USA, Cat# C11995500BT) supplemented with 10% heat-inactivated FBS (Gibco, USA, Cat# 26140-079) and 1% penicillin/streptomycin. Bone marrow-derived macrophages (BMMs) were isolated from the femur and tibia of WT or GPR65-KO mice (8–9 weeks) and cultured in minimum essential medium alpha ( $\alpha$ -MEM, Gibco, USA, Cat# C11095500BT)

containing 10% FBS, 1% penicillin/streptomycin (Solarbio, China, Cat# P1400) and 10 ng/ml murine macrophage colony stimulating factor (M-CSF, PeproTech, USA, Cat# 300-25) for 6 d. The non-tumorigenic mouse hepatocyte cell line AML12 cells (National Collection of Authenticated Cell Cultures, China) were cultured in DMEM/F-12 (Gibco, USA, Cat# C11330500BT) containing 10% FBS, 40 ng/ml dexamethasone (Sigma-Aldrich, USA, Cat# D4902), 1×insulin–transferrin–sodium selenite media supplement (ITS, Sigma-Aldrich, USA, Cat# I3146), 1% penicillin/streptomycin (Solarbio, China, Cat# P1400). Cells were treated with the GPR65 agonist BTB09089 (Maybridge, Belgium, Cat# BTB09089; or Otava, Ukraine, Cat# 14900668; 30 μmol/L), GPR65 inhibitor ZINC62678696 (Enamine, USA, Cat# EN300-261362; or Molport, Latvia, Cat# molport-019-671-510; 30 μmol/L), BAY 11-7082 (MCE, USA, Cat# HY-13453; 5 μmol/L), ammonium pyrrolidine dithiocarbamate (APDC, MCE, USA, Cat# HY-18738; 20 μmol/L), SP600125 (MCE, USA, Cat# HY-12041; 10 μmol/L), JNK inhibitor XVI (JNK-IN-8, Selleck, USA, Cat# S4901; 5 μmol/L), YM-254890 (Focus Biomolecules, USA, Cat# 10-1590; 1 μmol/L), BAPTA (MCE, USA, Cat# HY-100168, 10 μmol/L) or Compound C (MCE, USA, Cat# HY-13418A; 10 μmol/L). For acidic exposure, DMEM or α-MEM with 10% FBS was prepared by using biologic buffer [either 4-(2-hydroxyethyl)-1-piperazineethanesulfonic acid (HEPES), HCl or NaOH for pH 6.6, pH 8.2 and pH 7.2, respectively]. Cells were treated with the appropriate pH and the pH of the culture media was regularly monitored using an acid–base indicator (e.g., phenol red) and adjusted for maintenance. For co-culture experiment, HMs and RAW264.7 cells were treated as described in individual experiment. The centrifuged cell supernatant was filtered through 0.22 μm filtration and was finally collected as the conditioned medium (CM). The CM with 20 μg/ml transforming growth factor-β (TGF-β) neutralization antibody 1D11 (Thermo Fisher Scientific, USA, Cat# 16-9243-85; RRID: AB\_2573124) or mouse IgG, was used to treat primary HSCs.

#### Quantitative real-time reverse transcription-polymerase chain reaction (qRT-PCR)

RNA isolation and qRT-PCR were performed as previously reported [17–21]. The gene expression was normalized to housekeeping gene *GAPDH*, and fold change was determined utilizing the  $2^{-\Delta\Delta C_t}$  method. For cell-by-cell qPCR analysis, the data were analyzed based on *GAPDH* calibration and compared with normal HMs. The primer sequences for qRT-PCR are provided in Additional file 1: Table S2.

#### Western blotting

Protein isolation and Western blotting were performed as previously reported [17–21]. Antibodies used for Western blotting included collagen I (rabbit polyclonal, Abcam, USA, ab34710; RRID: AB\_731684; 1:1000; rabbit polyclonal, ABclonal, China, A1352; RRID: AB\_2760381; 1:1000; for tissues; rabbit polyclonal, Novus, USA, NB600-408 for cells; RRID: AB\_10000511; 1:2000), α-SMA (rabbit polyclonal, Abcam, USA, ab5694 for tissues; RRID: AB\_2223021; 1:1000; rabbit polyclonal, ABclonal, USA, A17910 for cells; RRID: AB\_2861755; 1:1000), tissue metalloproteinase inhibitor 1 (TIMP1, mouse monoclonal, Santa Cruz, USA, sc-21734; RRID: AB\_628359; 1:1000), matrix metalloproteinase 2 (MMP2, rabbit monoclonal, Abcam, USA, ab92536; RRID: AB\_10561597; 1:1000), vimentin (rabbit monoclonal, CST, USA, #5741; RRID: AB\_10695459; 1:1000), Bcl-2-associated X protein (BAX, rabbit polyclonal, Abcam, USA, ab32503; RRID: AB\_725631; 1:1000), cleaved caspase-3 (rabbit monoclonal, CST, USA, #9661; RRID: AB\_2341188; 1:1000), caspase-3 (rabbit polyclonal, CST, USA, #9662; RRID: AB\_331439; 1:1000), proliferating cell nuclear antigen (PCNA, rabbit monoclonal, CST, USA, #13110; RRID: AB\_263697; 1:1000), monocyte chemoattractant protein 1 (MCP-1, rabbit polyclonal, CST, USA, #2029; RRID: AB\_1264199; 1:1000), CD11b (rabbit monoclonal, Abcam, USA, ab133357; RRID: AB\_2650514; 1:1000), interleukin-1β (IL-1β, mouse monoclonal, CST, USA, #12242; RRID: AB\_2715503; 1:1000), lymphocyte antigen 6 complex, locus C (LY6C, rat monoclonal, Novus, USA, NBP2-00441; RRID: AB\_2909793; 1:1000), tumor necrosis factor-α (TNF-α, mouse monoclonal, Santa Cruz, USA, sc-52746; RRID: AB\_630341; 1:1000), p-IκB kinase (p-IKK, rabbit monoclonal, CST, USA, #2697; RRID: AB\_2079382; 1:1000), p-p65 (rabbit monoclonal, CST, USA, #3033; RRID: AB\_331284; 1:1000), p-inhibitor of κB α (p-IκBα, mouse monoclonal, CST, USA, #9246; RRID: AB\_2267145; 1:1000), IKK (rabbit monoclonal, Abcam, USA, ab178870; RRID: AB\_2924430; 1:1000), p65 (mouse monoclonal, Santa Cruz, USA, sc-8008; RRID: AB\_62801; 1:200), IκBα (mouse monoclonal, CST, USA, #4814; RRID: AB\_390781; 1:1000), p-mixed lineage kinase 3 (p-MLK3, rabbit polyclonal, Affinity Biosciences, USA, # AF8079; RRID: AB\_2840142; 1:1000), p-mitogen-activated protein kinase kinase 4 (p-MKK4, rabbit polyclonal, CST, USA, #9156; RRID: AB\_2297420; 1:1000), p-MKK7 (rabbit recombinant, Proteintech, USA, #80357-1-RR; RRID: AB\_2918891; 1:2000), p-JNK (rabbit monoclonal, CST, USA, #4668; RRID: AB\_823588; 1:1000), p-p44/42 (rabbit monoclonal, CST, USA, #4370; RRID: AB\_2315112; 1:1000), p-p38 (rabbit monoclonal, CST, USA, #4511; RRID: AB\_2139682; 1:1000), JNK (rabbit polyclonal, CST,



USA, #9252; RRID: AB\_2250373; 1:1000), p44/42 (rabbit monoclonal, CST, USA, #4695; RRID: AB\_390779; 1:1000), p38 (rabbit monoclonal, CST, USA, #8690; RRID: AB\_10999090; 1:1000), p-glycogen synthase kinase-3 $\beta$  (p-GSK-3 $\beta$ , rabbit monoclonal, CST, USA, #5558; RRID: AB\_10013750; 1:1000), p-protein kinase B (p-Akt, Ser473, rabbit monoclonal, CST, USA, #4060; RRID: AB\_231504; 1:1000), p-pyruvate dehydrogenase kinase 1 (p-PDK1, Ser241, rabbit monoclonal, CST, USA, #3438; RRID: AB\_2161134; 1:1000), p-phosphatase and tensin homologue (p-PTEN, Ser380, rabbit polyclonal, CST, USA, #9551; RRID: AB\_331407; 1:1000), p-c-Raf (Ser259, rabbit polyclonal, CST, USA, #9421; RRID: AB\_330759; 1:1000), Akt (pan) (rabbit monoclonal, CST, USA, #4691; RRID: AB\_915783; 1:1000), GAPDH (mouse monoclonal, Abcam, USA, ab8245; RRID: AB\_2107448; 1:8000). GAPDH was used as an internal control.

### Histology and immunohistochemistry (IHC)

Formalin-fixed paraffin-embedded slides were prepared for histopathological analysis and IHC as previously reported [17–21]. In brief, 5  $\mu$ m sections were stained with Sirius red staining, HE staining and Masson's trichrome staining. Sirius red staining was conducted using 0.1% Direct Red 80 (Sigma, USA, Cat# 365548) in 1.3% picric acid solution (Sigma, USA, Cat# 239801) for 45 min, before dehydrated with ethanol and xylene. For Masson's trichrome staining, slides were dewaxed, rehydrated, stained with hematoxylin (Thermo Fisher, USA, Cat# SH26500D) for 5 min. Then stained with fuchsin solution for 10 s, phosphomolybdic acid solution for 2 min and aniline blue solution for 1 min followed by washing with weak acid working solution for 1 min. For IHC analysis, sections of three mice for each group were analyzed. Antibodies used for immunohistochemistry included GPR65 (Novus, USA, NBP2-24487 for human; 1:100; AVIVA Systems Biology, USA, for mouse, OABF01813; 1:200), collagen I (Novus, USA, NB600-408; 1:100),  $\alpha$ -SMA (Abcam, USA, ab5694; 1:200), TGF- $\beta$  (Abcam, USA, ab66043; 1:100), BAX (Abcam, USA, ab32503; 1:250), cleaved caspase-3 (CST, USA, #9661; 1:200), PCNA (CST, USA, #13110; 1:1000), Ki67 (Abcam, USA, ab16667; 1:200), F4/80 (Invitrogen, USA, 14-4801-81; 1:50), IL-1 $\beta$  (CST, USA, #12242; 1:100), and LY6C (Novus, USA, NBP2-00441; 1:200). In addition, control IgG staining was included as a negative control.

### RNA-seq

Briefly, samples (12 liver tissues from WT, WT+BDL, GPR65-KO and GPR65-KO+BDL respectively,  $n=3$ ) were collected and lysed with TRIzol reagent. RNA was qualified by Agilent 2100 bioanalyzer (Thermo, USA) and subsequently screened on BGISEQ500

platform (BGI-Shenzhen, China). The threshold was fold change >2 and  $P$ -adj < 0.05. The sequencing data have been deposited in NCBI GEO database: GSE182235 (<https://www.ncbi.nlm.nih.gov/geo/query/acc.cgi?acc=GSE182235>).

### Statistical analysis

Data were expressed as means  $\pm$  SEM with at least three independent experiments, except where noted. All statistical analyses were conducted using GraphPad 9. Statistical analysis was conducted using either one-way analysis of variance (more than two groups) or Student's  $t$ -test (two group comparison), and  $P < 0.05$  indicates a significant difference.

Details on other methods are shown in the Additional file 1.

## Results

### GPR65 is increased in human and mouse hepatic fibrosis

To clarify the key GPCRs involved in hepatic fibrosis, we intersected the GPCRs gene set with our previous microarray data which were conducted in mouse normal and fibrotic liver tissues (GSE80601 and GSE89147) (Additional file 1: Fig. S1a–d). Five GPCRs (*C3ar1*, *Ccr2*, *Gpr65*, *P2ry6* and *P2ry14*) which are increased in fibrotic livers more than twofold have been identified (Additional file 1: Fig. S1e). Of note, CCR2 and C3AR1 have been reported to be related with hepatic inflammation and fibrosis [7, 22]. In the present study, we focused our attention on the role and mechanism of proton-sensing receptor GPR65 in hepatic fibrosis. We first examined GPR65 expression in the livers of human subjects without fibrosis, with mild or advanced fibrosis as diagnosed clinically and pathologically (Additional file 1: Fig. S2a). The hepatic level of GPR65 was markedly upregulated in the livers of subjects with fibrosis than it was in individuals with normal livers (Fig. 1a; Additional file 1: Fig. S2a). Moreover, GPR65 was correlated with the expression of TNF- $\alpha$ , IL-6 rather than collagen type I alpha 1 (COL1 $\alpha$ 1) and actin alpha 2, smooth muscle (ACTA2/ $\alpha$ -SMA) (Fig. 1b, c; Additional file 1: Fig. S2b, c). In line with our observation in human, GPR65 expression was considerably upregulated in the liver tissues of CCl<sub>4</sub>- and BDL-treated mice (Fig. 1d, e; Additional file 1: Fig. S2d). Moreover, HCs, HSCs, HMs and LSECs from olive oil-treated and CCl<sub>4</sub>-treated mice were isolated, and we found *Gpr65* was highly expressed in primary HMs, lowly expressed in HCs and minimally expressed in HSCs and LSECs (Fig. 1f). IHC-frozen for co-staining GPR65 with macrophage markers (CD68 for human, LY6C or F4/80 for mouse) and HSC marker  $\alpha$ -SMA in normal and fibrotic livers revealed that GPR65 was mainly expressed in HMs (Fig. 1g–i; Additional file 1: Fig. S2e). Consistently, the expression of *Gpr65* in

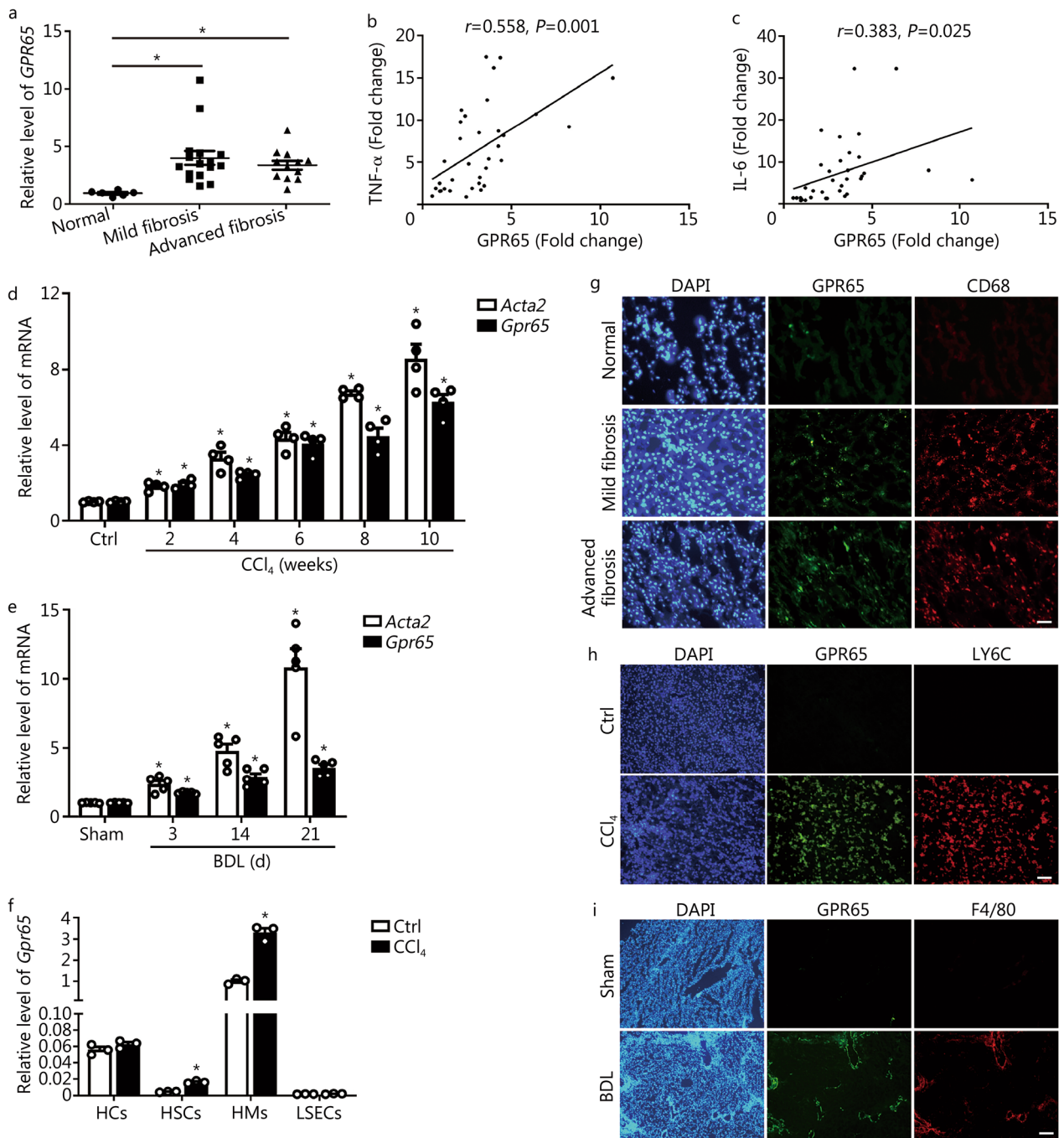


**Fig. 1** GPR65 is overexpressed in mouse and human hepatic fibrosis. **a** qRT-PCR was used to assess the mRNA level of *Gpr65* in liver tissues of human normal controls ( $n=6$ ), mild fibrosis ( $n=16$ ) and advanced fibrosis ( $n=12$ ). The correlations of GPR65, TNF- $\alpha$  (**b**) and IL-6 (**c**) were assessed using Pearson correlation analysis,  $n=34$ . **d** qRT-PCR was used to assess the expression of *Acta2* ( *$\alpha$ -SMA*) and *Gpr65* in livers from mice with CCl<sub>4</sub> treatment for different time points ( $n=4$ ). **e** qRT-PCR was used to assess the expression of *Acta2* and *Gpr65* in livers from mice treated with BDL for different time points ( $n=5$ ). **f** qRT-PCR was used to assess the expression of *Gpr65* in HCs, HSCs, HMs and LSECs that were isolated from livers of mice without or with CCl<sub>4</sub> treatment for 8 weeks ( $n=3$ ). **g** Representative IHC-frozen for co-staining GPR65 with macrophage marker CD68 in the liver of human normal controls, mild fibrosis and advanced fibrosis. Scale bar = 50  $\mu$ m. **h** Representative IHC-frozen for co-staining GPR65 with macrophage marker LY6C in the livers of mice without or with CCl<sub>4</sub> treatment for 8 weeks. Scale bar = 50  $\mu$ m. **i** Representative IHC-frozen for co-staining GPR65 with macrophage marker F4/80 in the livers of mice treated without or with BDL for 21 d. Scale bar = 125  $\mu$ m. \* $P < 0.05$  vs. Normal or Ctrl or Sham. BDL bile duct ligation, CCl<sub>4</sub> carbon tetrachloride, Ctrl control, HC hepatocyte, HM hepatic macrophage, HSC hepatic stellate cell, IHC immunohistochemistry, LSEC liver sinusoidal endothelial cell, qRT-PCR quantitative real-time reverse transcription-polymerase chain reaction, TNF- $\alpha$  tumor necrosis factor- $\alpha$ , IL-6 interleukin-6, LY6C lymphocyte antigen 6 complex

AML12, LX-2, RAW264.7, BMMs and HUVECs further confirmed that GPR65 is a macrophage-enriched GPCR (Additional file 1: Fig. S2f). In addition, the expression of *Gpr65* was increased in primary HMs isolated from mice treated with  $\text{CCl}_4$  for 1, 4 and 8 weeks, in line with the trend observed in *Il1 $\beta$*  and *Ly6c* (Additional file 1: Fig. S2g). However, our data revealed that TGF- $\beta$ , but not LPS, IFN- $\gamma$ , IL-4 and IL-10, promoted the expression of *Gpr65* in HMs (Additional file 1: Fig. S2h, i). Taken together, our results demonstrate that HMs-enriched GPR65 is upregulated in both human and mouse fibrotic livers, suggesting a role of GPR65 in the development of hepatic fibrosis.

### ***Gpr65* deficiency alleviates BDL-induced hepatic fibrosis**

To investigate the role of GPR65 in hepatic fibrosis in vivo, we generated GPR65-KO mice and subjected them to sham operation or BDL. *Gpr65* was successfully knocked out in livers of GPR65-KO mice compared to those of WT mice demonstrated by qRT-PCR and DNA sequencing, and BDL did not change the expression of *Gpr65* in the livers of GPR65-KO mice (Additional file 1: Fig. S3a). After 21 d of BDL, we performed RNA-seq to explore the effect of *Gpr65* deficiency on BDL-induced hepatic fibrosis (Fig. 2a). Firstly, our data confirmed that loss of *Gpr65* did not alter liver homeostasis, as demonstrated by changed expression of only four genes (*Gpr65*, *Rnf186*, *Acnat2* and *Creld2*) in the livers of GPR65-KO mice (Fig. 2a). Secondly, 2321 mRNAs were increased and 812 mRNAs were decreased in the BDL-treated WT mice, and the Kyoto Encyclopedia of Genes and Genomes (KEGG) pathway and Gene Ontology (GO) analysis demonstrated that BDL affected a list of genes related with cytokine-cytokine receptor interaction, ECM, ECM-receptor interaction, drug metabolism, fatty acid degradation, retinol metabolism, cell adhesion molecules, PI3K-Akt signaling and arachidonic acid metabolism (Additional file 1: Fig. S3b–d). Thirdly, only 592 mRNAs were increased and 104 mRNAs were decreased in the BDL-treated GPR65-KO mice, compared with GPR65-KO mice. Moreover, 182 mRNAs were increased and 358 mRNAs were decreased in the BDL-treated GPR65-KO mice, compared with the BDL-treated WT mice. Among these, 476 (137 mRNAs were increased and 339 mRNAs were decreased) out of 540 genes were also dysregulated in the BDL-treated WT mice (Fig. 2b, c). In addition, the KEGG pathway and GO analysis demonstrated that loss of *Gpr65* affected a series of genes related with retinol metabolism, arachidonic acid metabolism, cytokine-cytokine receptor interaction, ECM-receptor interaction, drug metabolism, PI3K-Akt signaling, NF- $\kappa$ B signaling and MAPK signaling, suggesting that *Gpr65* deficiency regulated BDL-induced hepatic metabolic dysfunction,

inflammation and fibrosis (Fig. 2d, e). To confirm this, we performed HE staining, Sirius red staining, Masson's trichrome staining and IHC for COL1 $\alpha$ 1 and  $\alpha$ -SMA, and the results revealed that loss of *Gpr65* significantly alleviated BDL-induced hepatic fibrosis (Fig. 2f; Additional file 1: Fig. S3e). Western blotting demonstrated that *Gpr65* deficiency obviously decreased BDL-induced up-regulation of COL1 $\alpha$ 1,  $\alpha$ -SMA, vimentin, MMP2 and TIMP1 (Fig. 2g). Consistently, qRT-PCR analysis showed that deficiency of *Gpr65* noticeably alleviated BDL-induced up-regulation of pro-fibrotic genes including *Acta2*, *Col1 $\alpha$ 1*, *Col3 $\alpha$ 1*, *Col12 $\alpha$ 1*, *Mmp2*, *Tgfb $\beta$ 1* and *Pdgfb $\beta$*  (Additional file 1: Fig. S3f). The hepatic hydroxyproline content in BDL-treated GPR65-KO mice was also markedly decreased compared to BDL-treated WT mice (Additional file 1: Fig. S3g), suggesting that loss of *Gpr65* significantly alleviated BDL-induced hepatic fibrosis. Furthermore, BDL-treated GPR65-KO mice exhibited significantly reduced hepatic injury and improved liver function than BDL-treated WT mice, as evidenced by HE staining, serum AST and ALT level, IHC and Western blotting for TGF- $\beta$ 1, BAX and cleaved caspase-3, and the mRNA level of genes involved in apoptosis (*Bad* and *Bax*) and drug/lipid/retinol metabolism (*Acnat2*, *Dhrs9*, *Nox2*, *Gpcpd1*, *Gsta2*, *Ugt2 $\beta$ 1* and *Sult1 $\beta$ 1*) in the livers (Fig. 2f; Additional file 1: Fig. S4a–f). However, the expression of proliferation-related genes, *Ki67* and *Pcna*, was not changed in GPR65-KO mice treated with BDL, compared with WT mice treated with BDL, suggesting that GPR65 may not affect proliferation during liver fibrogenesis (Additional file 1: Fig. S4c, d, f). Additionally, IHC, Western blotting and qRT-PCR results revealed that GPR65-KO mice treated with BDL also exhibited suppressed expression of pro-inflammatory genes (*Ly6c*, *Adgre1*, *Il1 $\beta$* , *Il6*, *Tnfa*, *Ccl2* and *Ccr2*) (Additional file 1: Fig. S4c, f, g). All these results demonstrate that *Gpr65* depletion ameliorates BDL-induced hepatic inflammation, injury and fibrosis in vivo.

### ***Gpr65* deficiency alleviates $\text{CCl}_4$ -induced hepatic fibrosis**

Considering the heterogeneity of hepatic fibrosis, we further examined GPR65 function with a  $\text{CCl}_4$ -induced hepatic fibrosis model. GPR65-KO mice or WT mice were treated with or without  $\text{CCl}_4$  for 8 weeks, and  $\text{CCl}_4$  did not change the level of *Gpr65* in the livers of GPR65-KO mice (Additional file 1: Fig. S5a, b). Similar to the results of the BDL model, compared to the WT mice, the GPR65-KO mice exhibited markedly decreased hepatic fibrosis following  $\text{CCl}_4$  treatment, as measured by HE staining, Sirius red staining, Masson's trichrome staining, IHC, Western blotting and qRT-PCR for pro-fibrotic genes, as well as liver hydroxyproline content (Fig. 3a–d). Furthermore, the degree



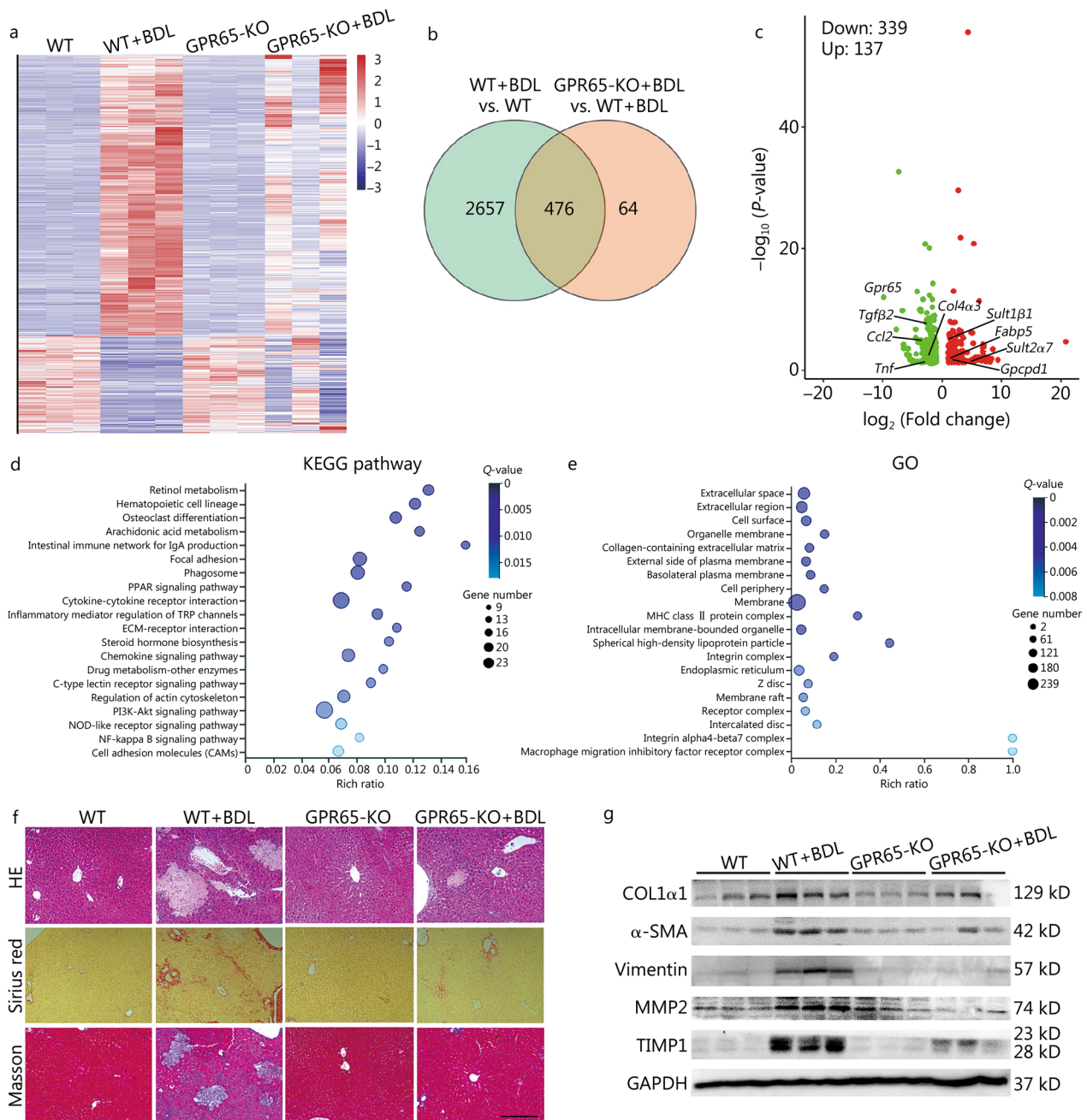


**Fig. 2** *Gpr65* deficiency alleviates hepatic fibrosis induced by BDL. **a** WT and GPR65-KO mice were divided into 4 groups: WT, WT + BDL, GPR65-KO and GPR65-KO + BDL. The significantly differentially expressed mRNAs were displayed by hierarchical cluster analysis: bright red, up-regulation; bright blue, down-regulation.  $n = 3/\text{group}$ . The Venn diagram (**b**), volcano map analysis (**c**), KEGG (**d**) and GO (**e**) analysis of differentially expressed mRNAs in WT mice treated with BDL, compared to WT mice, and GPR65-KO mice treated with BDL, compared to WT mice treated with BDL. **f** Hepatic fibrosis was evaluated by HE staining, Sirius red staining and Masson's trichrome staining. Scale bar = 400  $\mu\text{m}$ . **g** Western blotting was used to determine the protein level of COL1 $\alpha$ 1,  $\alpha$ -SMA, vimentin, MMP2 and TIMP1. BDL bile duct ligation, GO Gene Ontology, KEGG Kyoto Encyclopedia of Genes and Genomes, KO knockout, PPAR peroxisome proliferator activated receptor, TRP transient receptor potential, ECM extracellular matrix, NOD nucleotide oligomerization domain, MHC major histocompatibility complex, COL1 $\alpha$ 1 collagen type I alpha 1,  $\alpha$ -SMA  $\alpha$ -smooth muscle actin, MMP2 matrix metalloproteinase 2, TIMP1 tissue inhibitor of metalloproteinases 1



of CCl<sub>4</sub>-induced hepatic injury demonstrated by HE staining, serum ALT and AST level, and the level of genes related with apoptosis and metabolism in the livers were alleviated in GPR65-KO mice compared to WT controls (Fig. 3a, e, f; Additional file 1: Fig. S5c–f).

Additionally, IHC, qRT-PCR and Western blotting results revealed that the expression of pro-inflammatory genes was also markedly decreased in CCl<sub>4</sub>-treated GPR65-KO mice compared to CCl<sub>4</sub>-treated WT controls (Additional file 1: Fig. S5c, f, g).

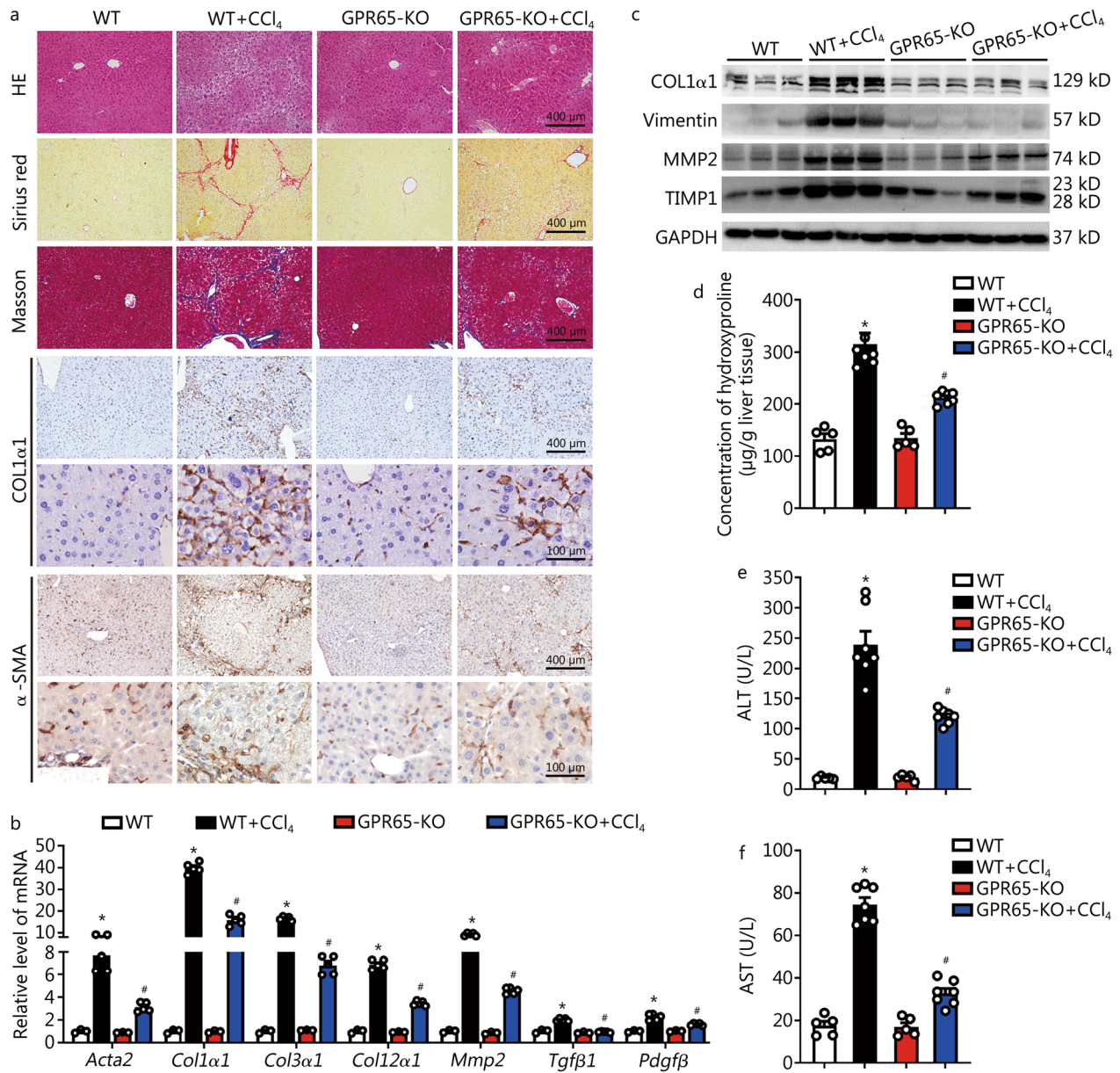


**Fig. 3** *Gpr65* deficiency alleviates hepatic fibrosis induced by CCl<sub>4</sub>. **a** WT and GPR65-KO mice were divided into 4 groups: WT, WT + CCl<sub>4</sub>, GPR65-KO and GPR65-KO + CCl<sub>4</sub>. Hepatic fibrosis was evaluated by HE staining, Sirius red staining, Masson's trichrome staining and IHC for COL1α1 and α-SMA. Scale bar = 100 µm for 40 × and 400 µm for 10 ×. **b** qRT-PCR was used to assess the mRNA level of *Acta2*, *Col1α1*, *Col3α1*, *Col12α1*, *Mmp2*, *Tgfb1* and *Pdgfb* (*n* = 3, 5, 3, 5). **c** Western blotting was used to determine the protein level of COL1α1, vimentin, MMP2 and TIMP1. **d** The content of hepatic hydroxyproline was quantified in livers of each group (*n* = 5, 7, 5, 7). Serum ALT (**e**) and AST (**f**) level were examined (*n* = 5, 7, 5, 7). \**P* < 0.05 vs. WT; #*P* < 0.05 vs. WT + CCl<sub>4</sub>. CCl<sub>4</sub> carbon tetrachloride, IHC immunohistochemistry, KO knockout, qRT-PCR quantitative real-time reverse transcription-polymerase chain reaction, COL1α1 collagen type I alpha 1, α-SMA α-smooth muscle actin, MMP2 matrix metalloproteinase 2, TIMP1 tissue inhibitor of metalloproteinases 1, ALT alanine aminotransferase, AST aspartate aminotransferase

As HMs are heterogeneous cell populations, consisting of liver-resident macrophage KCs and BMMs that are recruited from the circulation [16, 17], to further distinguish the roles of BMMs or KCs GPR65 in fibrosis development, we used irradiation and BMT to create chimeric mice with GPR65 inactivation only in bone marrow cells. Following treatment with CCl<sub>4</sub> thrice a week for 6 weeks, mice containing BMM *Gpr65* knockout exhibited attenuated hepatic fibrosis, inflammation and injury than WT/BMT-WT controls, as demonstrated by HE staining, Sirius red staining, Masson's trichrome staining, qRT-PCR, Western blotting, liver hydroxyproline content as well as serum ALT and AST level (Additional file 1: Fig. S6a–f). All these results demonstrate that *Gpr65* depletion alleviates CCl<sub>4</sub>-induced hepatic inflammation, injury and fibrosis in vivo, and the protective effect of *Gpr65* knockout is primarily mediated by BMMs.

#### GPR65 promotes macrophage M1 polarization

Given the evidences that macrophage-enriched GPR65 was increased in HMs from the fibrotic livers and *Gpr65* depletion ameliorated CCl<sub>4</sub>- and BDL-induced hepatic inflammation in vivo, we investigated the role of GPR65 on the polarization of macrophage in vitro. Thus, the expression of inflammation-related genes *Ccl2*, *Tnfa*, *Il1β*, *Il6*, *Ccl5*, *Ccr2*, *Nos2*, *Cd80*, *Cd86*, *Mrc1*, *Arg1*, *Cd163* and *Il10* was detected in HMs, which were isolated from GPR65-KO mice or WT mice. The results revealed that the level of pro-inflammatory genes including *Ccl2*, *Tnfa*, *Il1β*, *Il6*, *Ccl5* and *Nos2* was significantly decreased, whereas the level of anti-inflammatory gene *Mrc1*, *Arg1* and *Il10* was markedly increased in GPR65-KO HMs compared to WT controls (Fig. 4a). Similarly, confocal microscopy revealed that the level of TNF-α was decreased in GPR65-KO HMs (Fig. 4b). Moreover, mature TNF-α and IL-6 levels in the supernatant were assessed by enzyme-linked immunosorbent assay (ELISA), and the data indicated that the levels of TNF-α and IL-6 were downregulated in GPR65-KO HMs compared to WT controls (Fig. 4c). On the other hand, forced expression of GPR65 remarkably promoted the expression of the pro-inflammatory genes and the release of TNF-α and IL-6 in HMs as assessed by qRT-PCR, confocal microscopy and ELISA (Fig. 4d–f). Consequently, similar results were also obtained in BMMs and RAW264.7 cells (Additional file 1: Fig. S7, S8a–f). In addition, the expression of proliferation-related genes, *Pcna*, *Ki67*, *Ccnd1* and *Ccne1*, in GPR65-KO and GPR65-overexpressed HMs was also detected, and the data revealed that either knockdown or overexpression of *Gpr65* did not regulate the level of proliferation-related genes (Additional file 1: Fig. S8g, h). CCK-8 assay further confirmed that GPR65 did not affect macrophage

proliferation (Additional file 1: Fig. S8i). All these results indicate that GPR65 promotes macrophage M1 polarization in vitro.

#### Extracellular acidification differentially regulates macrophage polarization partly via GPR65

As GPR65 has been accepted as a proton-sensing GPCR and both anti-inflammatory and pro-inflammatory role of extracellular acidosis have been reported [11, 12], we explored the effect of extracellular acidosis on macrophage and, whether or not, it was dependent on GPR65. The expression of inflammation-related genes was examined in macrophage treated with various pH, including the physiological pH 7.4, the acidic pH 6.6 and the alkalic pH 8.2. Extracellular acidification promoted the level of the pro-inflammatory genes and the release of TNF-α and IL-6, while extracellular alkalization inhibited the level of these inflammation-related genes in HMs as assessed by qRT-PCR, confocal microscopy and ELISA (Additional file 1: Fig. S9a–c). Moreover, the upregulated levels of TNF-α, IL-6 and IL-1β in response to extracellular acidification were ablated in GPR65-KO HMs, suggesting that acidosis promoted M1 macrophage polarization of HMs partly via GPR65 (Additional file 1: Fig. S9d–f). However, both extracellular acidification and alkalization inhibited the level of the pro-inflammatory factors in BMMs, and the down-regulated expression of *Ccl2*, *Tnfa* and *Il6* in response to extracellular alkalization was not further decreased in GPR65-KO BMMs (Additional file 1: Fig. S10a–d), suggesting that acidosis had distinct effects on macrophage by various mechanisms and alkalosis inhibited M1 macrophage polarization of BMMs partly via GPR65. Subsequently, we also examined the role of extracellular acidosis on RAW264.7 cells, and the results revealed that extracellular acidification promoted the expression and release of the pro-inflammatory genes *Tnfa*, *Nos2*, *Ccl5*, *Cxcl10* rather than *Ccl2*, *Il1β* and *Il6*, while extracellular alkalization inhibited the expression and release of the pro-inflammatory factors as assessed by qRT-PCR, confocal microscopy and ELISA (Additional file 1: Fig. S11a–c). In addition, knockdown of *Gpr65* by two different specific siRNAs significantly abrogated overexpression of *Tnfa* and *Ccl5* in response to extracellular acidification (Additional file 1: Fig. S11c–e). All these results reveal that acidosis differentially regulates macrophage polarization and alkalosis inhibits M1 macrophage polarization partly via GPR65.

#### Effect of GPR65 exogenous agonist and inhibitor on macrophage polarization

It has been reported that BTB09089 is an allosteric agonist of GPR65 and ZINC62678696 functions as an allosteric inhibitor of GPR65 [23]. To further study the

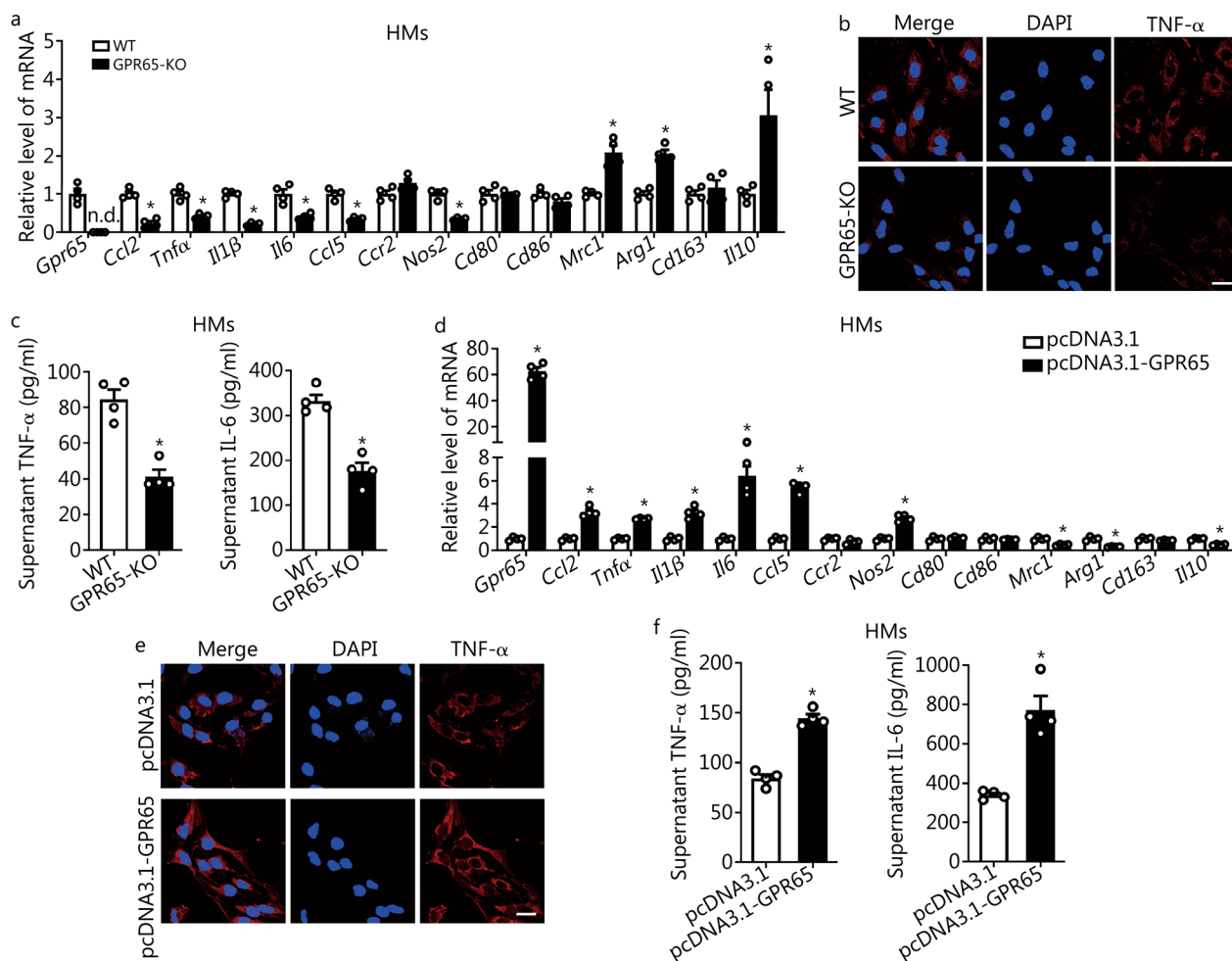


**Fig. 4** GPR65 promotes M1 macrophage polarization in vitro. **a** qRT-PCR was used to assess the mRNA level of *Gpr65*, *Ccl2*, *Tnfa*, *Il1β*, *Il6*, *Ccl5*, *Ccr2*, *Nos2*, *Cd80*, *Cd86*, *Mrc1*, *Arg1*, *Cd163* and *Il10* in HMs isolated from WT and GPR65-KO mice ( $n=4$ ). **b** The expression and location of TNF- $\alpha$  in HMs isolated from WT and GPR65-KO mice were assessed by confocal microscopy. Scale bar = 20  $\mu$ m. **c** TNF- $\alpha$  and IL-6 level in the supernatant of HMs isolated from WT and GPR65-KO mice were detected by ELISA ( $n=4$ ). HMs were transfected with pcDNA3.1 or pcDNA3.1-GPR65 for 48 h, qRT-PCR was used to assess the mRNA level of *Gpr65*, *Ccl2*, *Tnfa*, *Il1β*, *Il6*, *Ccl5*, *Ccr2*, *Nos2*, *Cd80*, *Cd86*, *Mrc1*, *Arg1*, *Cd163* and *Il10* ( $n=4$ ) (**d**); the expression and location of TNF- $\alpha$  was assessed by confocal microscopy (**e**). Scale bar = 20  $\mu$ m. TNF- $\alpha$  and IL-6 level in the supernatant were detected by ELISA ( $n=4$ ) (**f**). \* $P < 0.05$  vs. WT or pcDNA3.1. ELISA enzyme-linked immunosorbent assay, HM hepatic macrophage, KO knockout, qRT-PCR quantitative real-time reverse transcription-polymerase chain reaction, TNF- $\alpha$  tumor necrosis factor- $\alpha$ , IL-6 interleukin-6, n.d. not detected

function of GPR65 on macrophage polarization, the GPR65 exogenous agonist and inhibitor were used to treat HMs from GPR65-KO or WT mice. GPR65 inhibitor ZINC62678696 remarkably reduced the expression and release of the pro-inflammatory genes in HMs from WT mice and GPR65-overexpressed HMs, rather than HMs from GPR65-KO mice, suggesting that ZINC62678696 inhibited M1 macrophage polarization of HMs via GPR65 (Additional file 1: Fig. S12a–i). Unexpectedly, GPR65 agonist BTB09089 did not affect the expression of most inflammation-related genes at pH 7.4 and pH 6.6 (Additional file 1: Fig. S12a–c, j). Moreover, BTB09089 slightly enhanced the expression of

*Il6* in HMs at pH 8.2 (Additional file 1: Fig. S12k). However, BTB09089 obviously promoted the expression and release of the pro-inflammatory factors in BMMS at both physiological, acidic and alkalic pH, and *Gpr65* depletion ablated this overexpression in response to GPR65 agonist (Additional file 1: Fig. S13a–e). On the other hand, ZINC62678696 remarkably reduced the expression and release of the pro-inflammatory factors in BMMS (Additional file 1: Fig. S13a–c). The data were further confirmed in RAW264.7 cells shown in Additional file 1: Fig. S14a–e. Additionally, BTB09089 remarkably enhanced the level and release of the pro-inflammatory factors except *Il1β* and *Ccl5* in RAW264.7 cells at both



physiological and alkaline pH, and knockdown of *Gpr65* significantly abrogated overexpression of TNF- $\alpha$  and IL-6 in response to BTB09089 (Additional file 1: Fig. S14a, c, f, g). All these data demonstrate that ZINC62678696 delays, while BTB09089 promotes macrophage M1 polarization via GPR65.

#### **GPR65 promotes HSCs activation indirectly by paracrine secretion of TGF- $\beta$ from macrophage**

Activated HSCs are the central cellular player that promote ECM deposition in response to accumulated inflammatory signals [17, 19]. Thus, we explored the role of GPR65 on HSCs activation. We overexpressed GPR65 in mouse primary HSCs and LX-2 cells as its expression was quite low in these cells. Subsequently, the expression of the pro-fibrotic genes including *ACTA2*, *COL1 $\alpha$ 1*, *COL1 $\alpha$ 2*, *TIMP1*, *MMP2* and *TGF $\beta$ 1* was detected. The results revealed that only *Col1 $\alpha$ 2* and *Tgfb1* were upregulated by forced expression of GPR65 in HSCs, but not LX-2 cells (Additional file 1: Fig. S15a, b). Furthermore, both the endogenous and exogenous ligands of GPR65 did not regulate the level of these fibrotic genes in HSCs and LX-2 cells, suggesting that GPR65 was not involved in regulation of HSCs activation directly (Additional file 1: Fig. S15c–f). We, therefore, hypothesized that upregulated GPR65 in macrophage during hepatic fibrogenesis resulted in HMs M1 polarization, which subsequently induced HSCs activation. Hence, CM from control, GPR65-overexpressed, pH 6.6-treated or BTB09089-treated macrophage cells were used to incubate mouse primary HSCs. The results revealed that treatment with the CM from GPR65-overexpressed, pH 6.6- or BTB09089-treated macrophage cells markedly promoted the level of the pro-fibrotic genes, which was abrogated by TGF- $\beta$  neutralizing antibody 1D11 (Fig. 5a–e). Moreover, forced expression of GPR65, pH 6.6 and BTB09089 promoted, while knockdown of *Gpr65*, pH 8.2 and GPR65 antagonist ZINC62678696 remarkably reduced the expression of *Tgfb1* and *Tgfb3* in HMs and RAW264.7 cells (Fig. 5f–h; Additional file 1: Fig. S16a–h). As expected, supernatant TGF- $\beta$ 1 level in GPR65-overexpressed, pH 6.6-treated or BTB09089-treated HMs, BMMs and RAW264.7 cells was obviously increased (Fig. 5i–k; Additional file 1: Fig. S16i–s), suggesting that TGF- $\beta$ 1 is one of the factors derived from macrophage that induces HSCs activation. Altogether, our data demonstrate that GPR65 promotes the activation of HSCs via the signals derived from macrophage.

#### **GPR65 aggravates HCs damage through the signals derived from macrophage**

HCs damage or apoptosis has been widely recognized as a key initiator of fibrosis in ongoing hepatic injury

[20, 21]. Given the evidences that *Gpr65* deletion ameliorates CCl<sub>4</sub>- and BDL-induced hepatic damage in vivo, we explored the effect of GPR65 on HCs. We overexpressed GPR65 in HCs and AML12 cells as GPR65 was low expressed in HCs and minimally expressed in AML12 cells. Subsequently, the expression of apoptosis-related genes (*Bax*, *Bad*), inflammation-related genes (*Il1 $\beta$* , *Ccl2*) and metabolism-related genes (*Sult1 $\beta$ 1*, *Ugt2 $\beta$ 1*, *Cyp2 $\alpha$ 5*, *Cyp4 $\alpha$ 12*, *Gsta2*, *Nox2*, *Slc25 $\alpha$ 1*) was detected. The data demonstrated that forced expression of GPR65, the endogenous and exogenous ligands only slightly regulated the level of *Il1 $\beta$*  rather than apoptosis-, inflammation- and metabolism-related genes (Additional file 1: Fig. S17a–f), suggesting that GPR65 regulated HCs damage and metabolism mainly in an indirect manner. Considering that GPR65 promotes the level and release of pro-inflammatory genes and TGF- $\beta$ , which may subsequently act on HCs to induce damage, we also used CM from control, GPR65-overexpressed, pH 6.6-treated or BTB09089-treated macrophage cells to incubate mouse primary HCs. The results revealed that treatment with the CM from GPR65-overexpressed, pH 6.6-treated or BTB09089-treated macrophage cells obviously promoted HC damage as characterized by the overexpression of pro-apoptotic genes (*Bad* and *Bax*), the apoptosis-related morphologic changes, the increased level of cleaved caspase-3 and BAX (Additional file 1: Fig. S17g–k). All these data demonstrate that GPR65 aggravates HCs damage and metabolism dysfunction through the signals derived from macrophage.

#### **Targeting GPR65 alleviates HMs inflammation and fibrosis by suppressing the G $\alpha$ -Ca<sup>2+</sup>-JNK/NF- $\kappa$ B pathways**

To explore the downstream signaling of GPR65, we first examined the level of various G $\alpha$  subunits including *G $\alpha$ 11*, *G $\alpha$ q*, *G $\alpha$ i1*, *G $\alpha$ i2*, *G $\alpha$ i3*, *G $\alpha$ s* and *G $\alpha$ 13* in HMs, RAW264.7 cells and BMMs. The data revealed that all types of macrophages expressed *G $\alpha$ 11*, *G $\alpha$ q*, *G $\alpha$ i2*, *G $\alpha$ i3* and *G $\alpha$ 13*, but not *G $\alpha$ s*. Moreover, *G $\alpha$ i1* was expressed in HMs rather than RAW264.7 cells and BMMs (Additional file 1: Fig. S18a), reflecting the distinct responses to GPR65 of these cells. Next, specific siRNAs targeting *G $\alpha$ i2*, *G $\alpha$ i3*, *G $\alpha$ 11*, *G $\alpha$ 13* and *G $\alpha$ q* were used to knockdown these G $\alpha$  subunits in RAW264.7 cells treated with BTB09089, and subsequently the level of *Tnfa*, *Il6* and *Tgfb3* was detected. The data revealed that knockdown of *G $\alpha$ q* but not *G $\alpha$ i2*, *G $\alpha$ i3*, *G $\alpha$ 11* and *G $\alpha$ 13* attenuated BTB09089-induced up-regulation of *Tnfa*, *Il6* and *Tgfb3* (Additional file 1: Fig. S18b–f). Moreover, *G $\alpha$ q* silencing or *G $\alpha$ q* inhibitor YM254890 blocked GPR65 overexpression-, GPR65 agonist-, or pH6.6-induced up-regulation of IL-6, TNF- $\alpha$  and TGF- $\beta$  in RAW264.7 cells and HMs



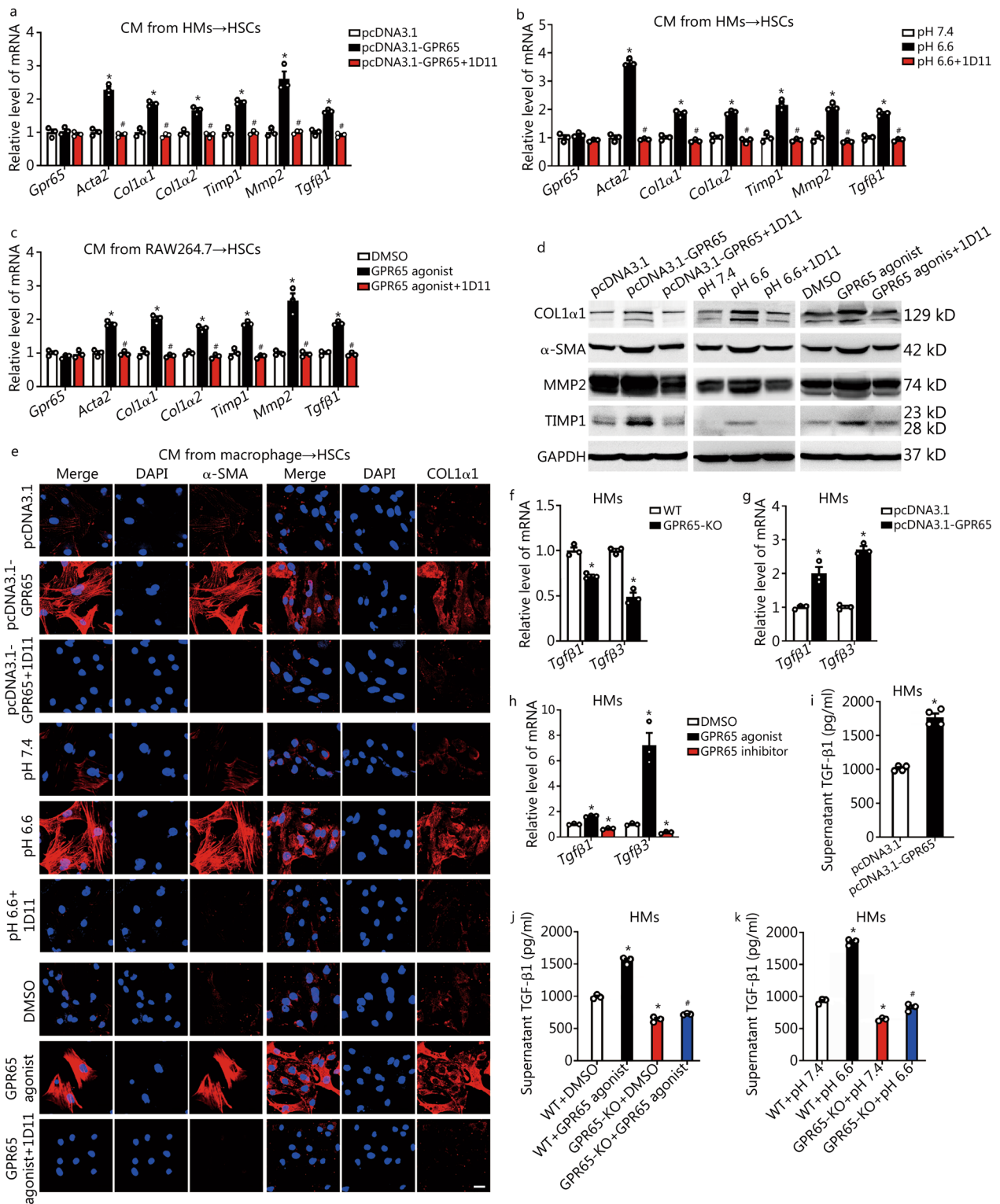


**Fig. 5** (See legend on next page.)

(See figure on previous page.)

**Fig. 5** GPR65 promotes HSCs activation indirectly by paracrine secretion of TGF- $\beta$  from macrophage. The CM from control, GPR65-overexpressed, pH 6.6-treated or GPR65 agonist-treated macrophage cells, with 20  $\mu\text{g}/\text{ml}$  TGF- $\beta$  neutralization antibody 1D11 or mouse IgG, were used to treat primary HSCs for 24 h. qRT-PCR was used to assess the mRNA level of *Gpr65*, *Acta2*, *Col1a1*, *Col1a2*, *Timp1*, *Mmp2* and *Tgfb1* (*n*=3) (**a-c**); Western blotting was used to determine the protein level of COL1 $\alpha$ 1,  $\alpha$ -SMA, MMP2 and TIMP1 (**d**); the expression and location of  $\alpha$ -SMA and COL1 $\alpha$ 1 was assessed by confocal microscopy (**e**). Scale bar = 20  $\mu\text{m}$ . qRT-PCR was used to assess the expression of *Tgfb1* and *Tgfb3* in GPR65-KO (**f**), *Gpr65*-overexpressed (**g**), or GPR65 agonist/inhibitor (**h**) treated HMs (*n*=3). **i** TGF- $\beta$ 1 level in the supernatant of HMs transfected with pcDNA3.1 or pcDNA3.1-GPR65 was detected by ELISA (*n*=4). HMs isolated from WT and GPR65-KO mice were treated with or without GPR65 agonist (**j**) or pH 6.6 (**k**) for 24 h, TGF- $\beta$ 1 level in the supernatant was detected by ELISA (*n*=3). \**P* < 0.05 vs. pcDNA3.1, pH 7.4, DMSO, WT, or WT + DMSO/pH 7.4; #*P* < 0.05 vs. pcDNA3.1-GPR65, pH 6.6, GPR65 agonist, or WT + GPR65 agonist/pH 6.6. CM conditioned medium, ELISA enzyme-linked immunosorbent assay, HM hepatic macrophage, HSC hepatic stellate cell, KO knockout, qRT-PCR quantitative real-time reverse transcription-polymerase chain reaction, COL1 $\alpha$ 1 collagen type I alpha 1,  $\alpha$ -SMA  $\alpha$ -smooth muscle actin, MMP2 matrix metalloproteinase 2, TIMP1 tissue inhibitor of metalloproteinases 1, TGF- $\beta$ 1 transforming growth factor- $\beta$ 1

(Additional file 1: Figs. S18g–k, S19). As the  $\text{Ca}^{2+}$ -AMPK signal is an important component of G $\alpha$ q signaling [24], BAPTA ( $\text{Ca}^{2+}$  chelator, 10  $\mu\text{mol}/\text{L}$ ) and Compound C (AMPK inhibitor, 10  $\mu\text{mol}/\text{L}$ ) were also applied in GPR65-overexpressed HMs, and the data revealed that BAPTA rather than Compound C rescinded GPR65 overexpression induced up-regulation of TGF- $\beta$ , TNF- $\alpha$  and IL-6 (Additional file 1: Fig. S20), suggesting that G $\alpha$ q- $\text{Ca}^{2+}$  mediates GPR65-induced up-regulation of TNF- $\alpha$ , IL-6 and TGF- $\beta$ .

Since the KEGG pathway and GO analysis indicated that *Gpr65* depletion affected a serial of genes related with PI3K-Akt, MAPK and NF- $\kappa$ B pathways (Fig. 2c–e), we firstly measured the level of p-IKK, p-I $\kappa$ B $\alpha$ , p-NF- $\kappa$ B p65, IKK, I $\kappa$ B $\alpha$ , NF- $\kappa$ B p65, p-MLK3 (Thr277/Ser281), p-MKK4 (Ser257/Thr261), p-MKK7 (Ser271/Thr275), p-JNK, p-p44/42, p-p38, JNK, p44/42, p38, p-GSK-3 $\beta$ , p-Akt (Ser473), p-PDK1, p-PTEN, p-c-Raf and Akt in liver tissues from BDL-/CCl $_4$ -induced WT and GPR65-KO mice. Western blotting analysis revealed that *Gpr65* depletion obviously ameliorated BDL- and CCl $_4$ -induced phosphorylation of IKK, I $\kappa$ B $\alpha$ , NF- $\kappa$ B p65, MLK3, MKK7 and JNK, while slightly inhibited phosphorylation of p38, Akt (Ser473) and c-Raf (Fig. 6a; Additional file 1: Fig. S21a). Unexpectedly, *Gpr65* depletion did not regulate BDL- and CCl $_4$ -induced phosphorylation of MKK4, p44/42, PDK1 and PTEN (Fig. 6a; Additional file 1: Fig. S21a). Moreover, forced expression of GPR65, pH 6.6 and BTB09089 significantly promoted, while knockout of *Gpr65*, pH 8.2 and ZINC62678696 reduced the phosphorylation of IKK, I $\kappa$ B $\alpha$ , NF- $\kappa$ B p65, MLK3, MKK7 and JNK in HMs and RAW264.7 cells (Fig. 6b; Additional file 1: Fig. S21b), suggesting that silencing GPR65 alleviated hepatic fibrosis and M1 macrophage polarization mainly through the JNK and NF- $\kappa$ B pathways. Subsequently, SP600125 and JNK-IN-8, the specific inhibitors of JNK, as well as BAY 11-7082 and APDC, the specific inhibitors of NF- $\kappa$ B, were

applied in GPR65-overexpressed, pH 6.6-treated or BTB09089-treated HMs and RAW264.7 cells, and the data revealed that SP600125 and JNK-IN-8 rather than BAY 11-7082 and APDC rescinded GPR65 overexpression, pH 6.6 and BTB09089-induced up-regulation of TGF- $\beta$ , while both JNK inhibitors and NF- $\kappa$ B inhibitors abrogated GPR65 overexpression, pH 6.6 and BTB09089-induced up-regulation of TNF- $\alpha$  and IL-6 (Fig. 6c–e; Additional file 1: Figs. S21c–e, S22). These data demonstrate that GPR65 overexpression, pH 6.6 and BTB09089 induce up-regulation of TNF- $\alpha$  and IL-6 via the G $\alpha$ q- $\text{Ca}^{2+}$ -JNK/NF- $\kappa$ B pathways, while promoting the expression of TGF- $\beta$  through the G $\alpha$ q- $\text{Ca}^{2+}$ -MLK3-MKK7-JNK pathway.

#### Pharmacological GPR65 inhibition alleviates CCl $_4$ -induced hepatic fibrosis

We next explored the therapeutic potential of targeting GPR65 in the development of hepatic fibrosis. ZINC62678696 (10  $\mu\text{g}/\text{g}$ ) was administered intraperitoneally every two days in the CCl $_4$ -treated or oil-treated mice 4 weeks after the first injection of CCl $_4$ . After 8 weeks of CCl $_4$  treatment, we tested whether the inhibition of GPR65 alleviated CCl $_4$ -induced hepatic fibrosis in vivo. As shown in Fig. 7a–d, GPR65 inhibition significantly attenuated CCl $_4$ -induced hepatic fibrosis, as evidenced by HE staining, Sirius red staining, Masson's trichrome staining, IHC, Western blotting and qRT-PCR for pro-fibrogenic genes, as well as liver hydroxyproline content. Moreover, the degree of CCl $_4$ -induced hepatic injury, demonstrated by serum ALT and AST level, HE staining, IHC, and the level of genes related with apoptosis and metabolism in the livers, was alleviated by GPR65 inhibitor in the CCl $_4$ -treated mice (Fig. 7a, e, f; Additional file 1: Fig. S23a–d). Additionally, the CCl $_4$ -induced hepatic expression of pro-inflammatory genes, as demonstrated by IHC, Western blotting and qRT-PCR, was also significantly reduced by GPR65 inhibitor in vivo (Additional file 1: Fig. S23b, d, e), indicating that GPR65

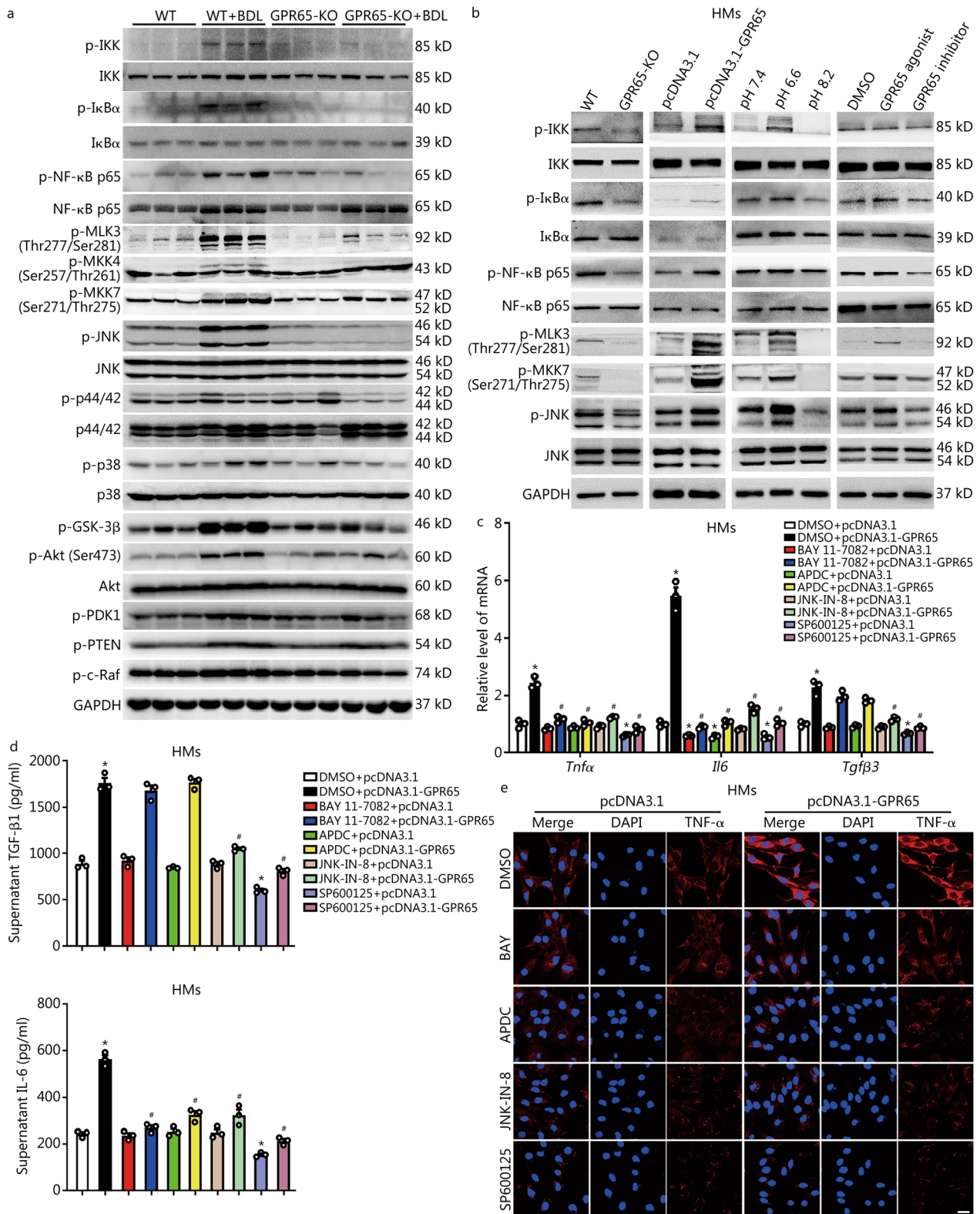


**Fig. 6** (See legend on next page.)



(See figure on previous page.)

**Fig. 6** Targeting GPR65 alleviates hepatic macrophage inflammation and fibrosis by suppressing the JNK/NF- $\kappa$ B pathways. **a** Western blotting was used to determine the level of p-IKK, p-I $\kappa$ B $\alpha$ , p-NF- $\kappa$ B p65, IKK, I $\kappa$ B $\alpha$ , NF- $\kappa$ B p65, p-MLK3, p-MKK4, p-MKK7, p-JNK, JNK, p-p44/42, p44/42, p-p38, p38, p-GSK-3 $\beta$ , p-Akt, Akt, p-PDK1, p-PTEN and p-c-Raf in liver tissues from WT, WT + BDL, GPR65-KO and GPR65-KO + BDL mice. **b** Western blotting was used to determine the level of p-IKK, IKK, p-I $\kappa$ B $\alpha$ , I $\kappa$ B $\alpha$ , p-p65, p65, p-MLK3, p-MKK7, p-JNK and JNK in GPR65-KO, GPR65-overexpressed, various pH-treated and GPR65 agonist/inhibitor-treated HMs. The specific inhibitors of JNK, SP600125 (10  $\mu$ mol/L) and JNK-IN-8 (5  $\mu$ mol/L), as well as the specific inhibitors of NF- $\kappa$ B, BAY 11-7082 (5  $\mu$ mol/L) and APDC (20  $\mu$ mol/L), were used to treat GPR65-overexpressed HMs for 24 h, and qRT-PCR was used to assess the expression of *Tnfa*, *Il6* and *Tgfb3* ( $n = 3$ ) (**c**); TGF- $\beta$ 1 and IL-6 level in the supernatant were detected by ELISA ( $n = 3$ ) (**d**); the expression and location of TNF- $\alpha$  was assessed by confocal microscopy (**e**). Scale bar = 20  $\mu$ m. \* $P < 0.05$  vs. DMSO + pcDNA3.1; # $P < 0.05$  vs. DMSO + pcDNA3.1-GPR65. CCl<sub>4</sub> carbon tetrachloride, BDL bile duct ligation, ELISA enzyme-linked immunosorbent assay, HM hepatic macrophage, KO knockout, qRT-PCR quantitative real-time reverse transcription-polymerase chain reaction, IKK inhibitor of  $\kappa$ B kinase, I $\kappa$ B $\alpha$  inhibitor of  $\kappa$ B  $\alpha$ , NF- $\kappa$ B p65 nuclear factor  $\kappa$ B p65 subunit, MLK3 mixed lineage kinase 3, MKK4 mitogen-activated protein kinase kinase 4, MKK7 mitogen-activated protein kinase kinase 7, JNK c-Jun N-terminal kinase, GSK-3 $\beta$  glycogen synthase kinase 3 $\beta$ , Akt protein kinase B, PDK1 pyruvate dehydrogenase kinase 1, PTEN phosphatase and tensin homolog, c-Raf c-rapidly accelerated fibrosarcoma, TGF- $\beta$ 1 transforming growth factor- $\beta$ 1, IL-6 interleukin-6, TNF- $\alpha$  tumor necrosis factor- $\alpha$

inhibitor has the potential for clinical transformation in the treatment of hepatic fibrosis. Finally, Western blotting results showed that GPR65 inhibitor significantly blocked CCl<sub>4</sub>-induced phosphorylation of IKK, I $\kappa$ B $\alpha$ , NF- $\kappa$ B p65, MLK3, MKK7 and JNK rather than MKK4, p44/42, p38, GSK-3 $\beta$  and PDK1, suggesting that GPR65 inhibition attenuates the CCl<sub>4</sub>-induced activation of JNK/NF- $\kappa$ B signaling (Additional file 1: Fig. S24a). Taken together, the results reveal that pharmacological GPR65 inhibition alleviates CCl<sub>4</sub>-induced hepatic inflammation, injury and fibrosis in vivo.

## Discussion

Cirrhosis is the end stage of progressive hepatic fibrosis resulted from a sustained injury repair in response to chronic hepatic injury [1]. Despite continuous progress that has been made during the last thirty years in exploring the cellular and molecular mechanisms of hepatic fibrosis and cirrhosis. However, the prevalence of hepatic cirrhosis is still surging and no specific drugs have been approved. Therefore, the need to develop promising drug targets and corresponding therapeutic molecules remains urgent. GPCRs, the largest family of transmembrane receptors mediating the majority of cellular responses, play a vital role in various pathophysiological processes including cardiovascular diseases, cancer and inflammation-related diseases [6, 25, 26]. Due to their cell membrane localization, diversified expression and clear binding pockets, GPCRs have become attractive drug targets and the sales of GPCR targeted drugs account for more than 27% of the global market share [6]. As GPCRs are widely expressed in various cells, and the functions of certain GPCRs in HCs, HSCs and HMs during hepatic fibrosis remain controversial [7], suggesting that developing therapeutics drugs targeting GPCRs for hepatic fibrosis without compromising other physiological functions is a great challenge. In this study, we

have identified that the proton-sensing receptor GPR65, which is a macrophage-enriched GPCR, is upregulated in both human and mouse fibrotic livers as well as primary HMs from fibrotic livers of mice. Both in vivo and in vitro data provided convincing evidences that silencing or the antagonist of GPR65 inhibited, while overexpression or the application of the endogenous and exogenous agonist of this receptor enhanced the expression and release of TNF- $\alpha$ , IL-6 and TGF- $\beta$ , all of which promoted the activation of HSCs and the damage of HCs, and subsequently aggravate BDL- and CCl<sub>4</sub>-induced hepatic inflammation, injury and fibrosis. Mechanistically, our results demonstrated that GPR65 overexpression, the acidic pH and exogenous GPR65 agonist induced up-regulation of TNF- $\alpha$  and IL-6 via the G $\alpha$ q-Ca<sup>2+</sup>-JNK/NF- $\kappa$ B pathways, while promoting the expression of TGF- $\beta$  through the G $\alpha$ q-Ca<sup>2+</sup>-MLK3-MKK7-JNK pathway. These results suggest that pharmacological inhibition of GPR65 could protect against hepatic fibrosis, thus providing new cues for harnessing hepatic fibrosis by developing innovative therapeutic approaches based on the GPR65-G $\alpha$ q-Ca<sup>2+</sup>-JNK/NF- $\kappa$ B pathways (Fig. 8).

Although the expression of human GPR65 was not correlated with the degree of fibrosis as demonstrated by the expression of GPR65 was not further increased with the progression of fibrosis and no correlations were found with COL1 $\alpha$ 1 and ACTA2 (Fig. 1a; Additional file 1: Fig. S2b, c). However, the hepatic level of human GPR65 was correlated with TNF- $\alpha$ , IL-6, both of which reflect the degree of inflammation (Fig. 1b, c). The reason for this is, on one hand, that HMs-enriched GPR65 was not directly involved in the regulation of the activation of HSCs as well as the injury of HCs, but acted on HSCs and HCs through the signals derived from HMs. On the other hand, human hepatic fibrosis is a complex condition influenced by a multitude of factors, including genetic variations, environmental factors, and co-existing



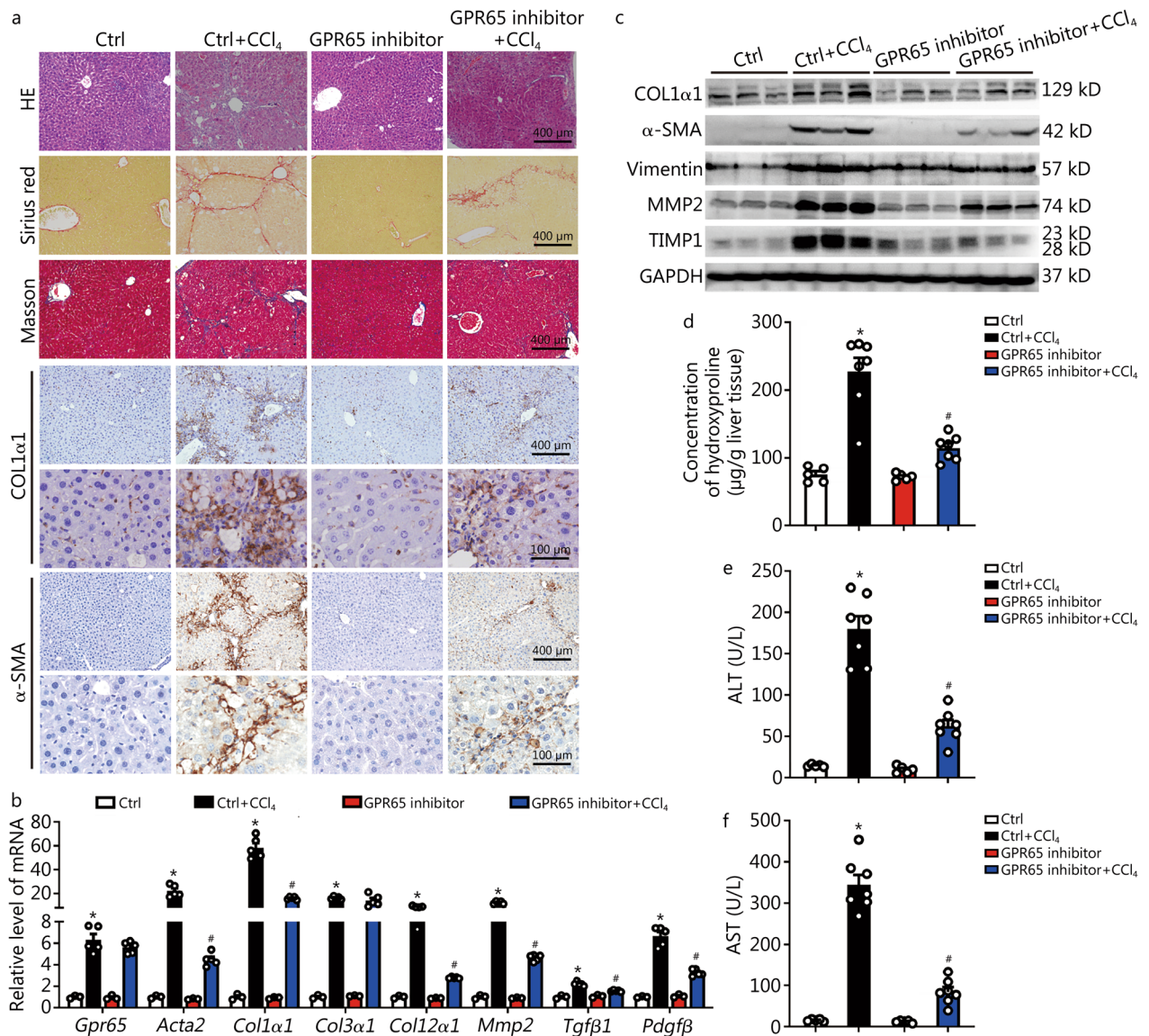


**Fig. 7** Pharmacological GPR65 inhibition alleviates hepatic fibrosis induced by CCl<sub>4</sub>. **a** BALB/c mice were divided into 4 groups randomly: Ctrl, Ctrl+CCl<sub>4</sub>, GPR65 inhibitor and GPR65 inhibitor+CCl<sub>4</sub>. The GPR65 inhibitor (10 mg/kg) was administered 4 weeks after the first CCl<sub>4</sub> injection. Mice were administered CCl<sub>4</sub> for 8 weeks. Hepatic fibrosis was evaluated by HE staining, Sirius red staining, Masson's trichrome staining and IHC for COL1α1 and α-SMA. Scale bar = 100 μm for 40× and 400 μm for 10×. **b** qRT-PCR was used to assess the mRNA level of *Gpr65*, *Acta2*, *Col1a1*, *Col3a1*, *Col12a1*, *Mmp2*, *Tgfb1* and *Pdgfb* (n = 3, 5, 3, 5). **c** Western blotting was used to determine the protein level of COL1α1, α-SMA, vimentin, MMP2 and TIMP1. **d** The content of hepatic hydroxyproline was quantified in livers of each group (n = 5, 7, 5, 7). Serum ALT (**e**) and AST (**f**) were examined (n = 5, 7, 5, 7). \*P < 0.05 vs. Ctrl; #P < 0.05 for vs. Ctrl + CCl<sub>4</sub>. CCl<sub>4</sub> carbon tetrachloride, Ctrl control, IHC immunohistochemistry, qRT-PCR quantitative real-time reverse transcription-polymerase chain reaction, COL1α1 collagen type I alpha 1, α-SMA α-smooth muscle actin, MMP2 matrix metalloproteinase 2, TIMP1 tissue inhibitor of metalloproteinases 1, ALT alanine aminotransferase, AST aspartate aminotransferase

comorbidities. These factors could contribute to the heterogeneity and variability observed in fibrosis progression and GPR65 expression patterns among human patients. Interestingly, based on the fact that GPR65-KO mice were not abnormal in size, appearance and mating at the age of 12 months, together with the finding

that both GPR65-KO mice and the application of GPR65 inhibitor in vivo did not exhibit any functional and morphological abnormalities (data not shown), it suggests that GPR65 is a promising and specific drug target for hepatic fibrosis, cirrhosis, or even inflammation-related diseases.

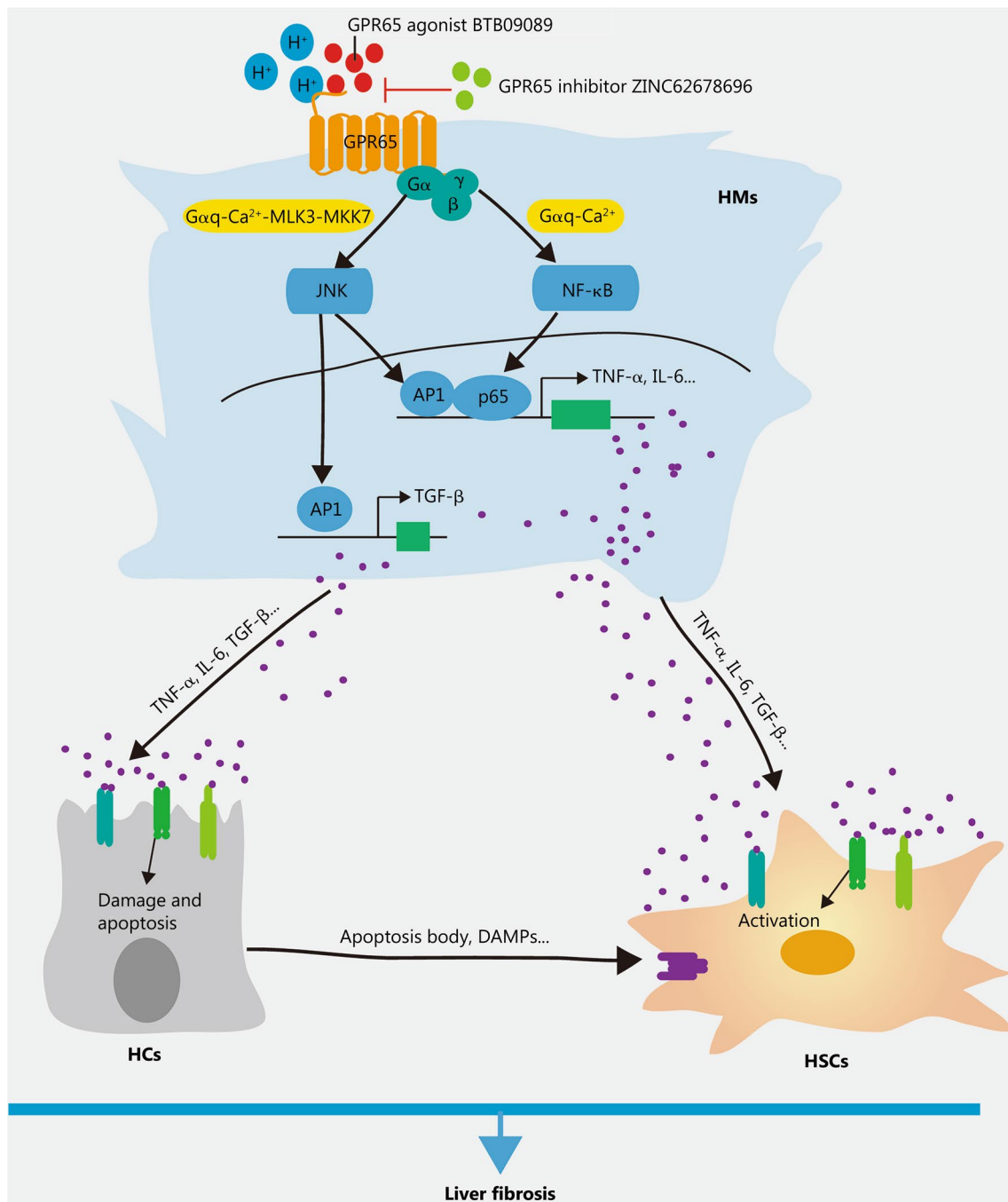


**Fig. 8** Schematic diagram illustrating the function and mechanism of GPR65 in the progression of liver inflammation and fibrosis. Upon liver injury, increased or activated HMs-enriched GPR65 induces up-regulation of TNF- $\alpha$  and IL-6 via the G $\alpha$ q-Ca<sup>2+</sup>-JNK/NF- $\kappa$ B pathways, while promoting the expression of TGF- $\beta$  through the G $\alpha$ q-Ca<sup>2+</sup>-MLK3-MKK7-JNK pathway in HMs, thus resulting in the damage of HCs and the activation of HSCs, and subsequently aggravate BDL- and CCl<sub>4</sub>-induced liver inflammation, injury and fibrosis. In addition, pharmacological inhibition of GPR65 can block this process. BDL bile duct ligation, CCl<sub>4</sub> carbon tetrachloride, HC hepatocyte, HM hepatic macrophage, HSC hepatic stellate cell, MLK3 mixed lineage kinase 3, MKK7 mitogen-activated protein kinase kinase 7, NF- $\kappa$ B nuclear factor  $\kappa$ B, JNK c-Jun N-terminal kinase, AP1 activator protein 1, TNF- $\alpha$  tumor necrosis factor- $\alpha$ , IL-6 interleukin-6, TGF- $\beta$  transforming growth factor- $\beta$ , DAMPs damage-associated molecular patterns

GPCRs are integral membrane proteins composed of seven transmembrane  $\alpha$ -helices. Upon binding of activating ligands or agonists, a conformational change occurs in the GPCR, allowing it to interact with a heterotrimeric G protein and promote the exchange of GTP for GDP on the  $G\alpha$  subunit [27, 28]. In a simplified model, agonist binding stabilizes the receptor in an active conformation, enabling its interaction with intracellular partners [5]. In our study, we observed that overexpression of GPR65 alone, in the absence of agonist or acid, leads to the up-regulation of pro-inflammatory cytokines (Fig. 4d-f). The underlying mechanism that overexpression of GPR65 induces cytokine production is that there is a certain level of proton concentration in the normal cell culture medium, which is enough or partially to contribute to the activity of overexpressed GPR65 with the exception of baseline activity of the receptor. These findings are in line with previous reports that many GPCRs exhibit a basal level of GTP exchange activity in the absence of an exogenous ligand and often display a degree of basal or constitutive signaling when overexpressed [5, 29].

Hepatic fibrosis is a reversible pathological process, and its reversibility is determined by the microenvironment created by the interaction among HMs, HCs and HSCs as well as pro-fibrotic signals [1, 30]. Emerging evidences demonstrated that inflammation is an important driver of fibrosis [1, 17, 19, 21, 31]. Interestingly, our data revealed that GPR65 does not affect HM number by the following evidences. Firstly, the results of RNA-seq analysis revealed that loss of *Gpr65* results in changed expression of only four genes in the livers of GPR65-KO mice (Fig. 2a), indicating that GPR65-KO did not alter the number of HMs in the normal liver condition. Secondly, the expression of proliferation-related genes *Pcna* and *Ki67* did not significantly change in GPR65-KO mice compared to WT controls, as well as in  $CCl_4$ - and BDL-treated GPR65-KO mice compared to  $CCl_4$ - and BDL-treated WT controls (Additional file 1: Figs. S4c, d, f and S5c, d, f). Thirdly, gain- and loss-of-function experiments in vitro confirmed that overexpression and knockout of *Gpr65* did not regulate the expression of proliferation-related genes (Additional file 1: Fig. S8g-i). However, we found that F4/80 and LY6C positive cells are decreased in GPR65-KO mice after BDL and  $CCl_4$  treatment (Additional file 1: Figs. S4c, d, f and S5c, d, f). As the increased number of HMs during liver fibrosis was caused by recruitment from blood and self-proliferation. Therefore, we believe that F4/80 and LY6C positive cells are decreased in GPR65-KO mice after BDL and  $CCl_4$  treatment may be a result of reduced recruited macrophage or the consequence of decreased liver fibrosis.

It is well-known that local acidosis, which is attributed partly to increased lactate production by the inflammatory cells, HCs and gut cells, is the hallmark of many

chronic inflammatory diseases including fibrosis and tumor microenvironment [9, 32, 33]. Cells sensing extracellular acidosis have several mechanisms. Ion channels including transient receptor potential V1 and acid-sensing ion channel, mainly expressed on sensory neurons, represent one sensing mechanism [34]. GPR65 together with GPR4, GPR68, and GPR132, all of which identified as proton-sensing GPCRs, represents another type of proton sensing mechanisms [9]. In the present study, we detected these proton-sensing GPCRs in normal and fibrotic liver tissues, and the results revealed that *Gpr4* and *Gpr65* were expressed in livers and only *Gpr65* was overexpressed in fibrotic livers, indicating a crucial role of this receptor in fibrogenesis (Additional file 1: Fig. S24b). To date, both anti-inflammatory and pro-inflammatory activities of GPR65 in response to acidosis have been reported, for instance, loss of *Gpr65* promotes the expression of pro-inflammatory factors, as well as colonic macrophage and neutrophil infiltration in the acute and chronic inflammatory bowel disease [11, 14, 35]. It has been also reported that GPR65 partly mediates the extracellular acidification-induced up-regulation of pro-inflammatory cytokine production in mouse macrophages. Furthermore, GPR65 can also stimulate the inflammatory response and is a member of the module that co-varies with pro-inflammatory genes [36]. Several studies revealed that blocking GPR65 expression and function was related with decreased level of pro-inflammatory cytokines including TNF- $\alpha$ , IL-17 and IFN- $\gamma$ , reduced synovial inflammation, eosinophil viability and microglial activation [12, 14, 37]. However, the precise impact of GPR65 in response to local acidosis on HMs inflammation, HCs damage, HSCs activation, and hepatic fibrogenesis remains unclear. Our study revealed that extracellular alkalization inhibited the level of the pro-inflammatory genes in HMs, BMMs and RAW264.7 cells, while extracellular acidification promoted the expression and release of the pro-inflammatory genes via GPR65 in HMs and RAW264.7 cells rather than BMMs. Moreover, the pro-inflammatory genes upregulated in HMs and RAW264.7 cells are not absolutely identical. To explain the discrepancy, we detected the level of proton-sensing GPCRs and the downstream various  $G\alpha$  subunits in macrophages, and the results revealed that *Gpr4* and *Gpr65* were highly expressed in HMs, while both BMMs and RAW264.7 cells mainly expressed *Gpr65* and *Gpr132*, followed by moderate expression of *Gpr4* in RAW264.7 cells (Additional file 1: Fig. S24c). In addition, our data showed that all types of macrophages expressed *Gai2*, *Gai3*, *Gaq*, *Ga11* and *Ga13*, but not *Gas*, and *Gai1* was expressed in HMs rather than BMMs and RAW264.7 cells (Additional file 1: Fig. S18a). The different expression patterns of GPCRs and  $G\alpha$  subunits may partially reflect the distinct

responses to acidosis in HMs, BMMs and RAW264.7 cells. Surprisingly, extracellular acidification does not regulate the level of the fibrotic-related genes in HSCs and the expression of apoptosis-, inflammation- and metabolism-related genes, except for *Nox2* and *Slc25a1*, in HCs, suggesting that acidosis does not regulate HSCs activation and HCs damage and metabolism directly. Further investigation on the effect of acid–base microenvironment during liver fibrogenesis is needed.

## Conclusions

In summary, our results provide convincing evidences that the HMs-enriched proton-sensing GPR65 is involved in hepatic fibrosis in both mice and human. Given the role of GPR65 as a physiologic integrator of the microenvironment (especially inflammation condition), these data provide insight into the molecular mechanisms by which the acidosis-activated GPR65 may contribute to the progression of fibrosis. It also brings some understanding of the anti-inflammatory effects of the GPR65 inhibitor, which may open novel avenues of research for drug development in the treatment of hepatic fibrosis and inflammation-related diseases.

## Abbreviations

BDL	Bile duct ligation
BMM	Bone marrow-derived macrophage
BMT	Bone marrow transplantation
cAMP	Cyclic AMP
CCl <sub>4</sub>	Carbon tetrachloride
CM	Conditioned medium
CREB	CAMP-responsive-element-binding protein
ECM	Extracellular matrix
ELISA	Enzyme-linked immunosorbent assay
FBS	Fetal bovine serum
GO	Gene Ontology
GPCR	G-protein coupled receptor
HC	Hepatocyte
HEPES	4-(2-Hydroxyethyl)-1-piperazineethanesulfonic acid
HM	Hepatic macrophage
HSC	Hepatic stellate cell
IHC	Immunohistochemistry
KC	Kupffer cells
KEGG	Kyoto Encyclopedia of Genes and Genomes
KO	Knockout
LSEC	Liver sinusoidal endothelial cell
PKA	Protein kinase A
PKC	Protein kinase C
PLC-β	Phospholipase C-β
qRT-PCR	Quantitative real-time reverse transcription-polymerase chain reaction

## Supplementary Information

The online version contains supplementary material available at <https://doi.org/10.1186/s40779-023-00494-4>.

**Additional file 1:** Materials and methods. **Table S1** Clinical characteristics of patients. **Table S2** Quantitative real-time reverse transcription-polymerase chain reaction (qRT-PCR) primers for analysis of transcript

levels. **Table S3** Cloning primers for GPR65. **Table S4** siRNA sequences. **Fig. S1** Identification of GPR65 during hepatic fibrosis. **Fig. S2** GPR65 is enriched in hepatic macrophage. **Fig. S3** *Gpr65* deficiency alleviates BDL-induced hepatic fibrosis. **Fig. S4** *Gpr65* deficiency alleviates BDL-induced hepatic injury and inflammation. **Fig. S5** *Gpr65* deficiency ameliorates CCl<sub>4</sub>-induced hepatic injury and inflammation. **Fig. S6** *Gpr65* deficiency in BMMs ameliorates CCl<sub>4</sub>-induced hepatic fibrosis, injury and inflammation. **Fig. S7** GPR65 promotes BMMs M1 polarization. **Fig. S8** GPR65 promotes RAW264.7 cell M1 polarization. **Fig. S9** Extracellular pH differentially regulates HMs polarization partly via GPR65. **Fig. S10** Extracellular pH differentially regulates BMMs polarization partly via GPR65. **Fig. S11** Extracellular pH differentially regulates RAW264.7 cells polarization partly via GPR65. **Fig. S12** Effect of GPR65 exogenous agonist and inhibitor on HMs polarization. **Fig. S13** Effect of GPR65 exogenous agonist and inhibitor on BMMs polarization. **Fig. S14** Effect of GPR65 exogenous agonist and inhibitor on RAW264.7 cells polarization. **Fig. S15** GPR65 is not involved in regulation of HSCs activation directly. **Fig. S16** GPR65 promotes the expression and release of TGF-β. **Fig. S17** GPR65 aggravates HCs damage through the signals derived from macrophage. **Fig. S18** Targeting GPR65 alleviates inflammation via Gαq. **Fig. S19** Targeting GPR65 alleviates hepatic macrophage inflammation via Gαq. **Fig. S20** Targeting GPR65 alleviates hepatic macrophage inflammation via Ca<sup>2+</sup> rather than AMPK. **Fig. S21** Targeting GPR65 alleviates hepatic macrophage inflammation by suppressing the JNK/NF-κB pathways. **Fig. S22** Targeting GPR65 alleviates inflammation by suppressing the JNK/NF-κB pathways. **Fig. S23** Pharmacological GPR65 inhibition alleviates CCl<sub>4</sub>-induced hepatic injury and inflammation. **Fig. S24** Targeting GPR65 alleviates hepatic fibrosis by suppressing the JNK/NF-κB pathways.

**Additional file 2:** The GPCRs gene set.

## Acknowledgements

Not applicable.

## Authors' contributions

WH, KZ and TH conceived the study. MXZ, KZ, XXM, JZ, JJW, YFH, YHL, SCZ, ZMS and LNZ performed experiments. MXZ, KZ, XXM, JZ and WH analyzed the data. WH, KZ and TH supervised the study. KZ draft the initial version of manuscript. WH, TH, MXZ, XXM, JZ and ZMS provided critical revision of the manuscript. All authors read and approved the final draft for publication.

## Funding

This work was supported by the National Natural Science Foundation of China (32171125, 81971331 and 82170630).

## Availability of data and materials

All the data supporting the findings of this study are available within the article and its Supplementary Information files or from the corresponding author upon reasonable request.

## Declarations

### Ethics approval and consent to participate

Experiments involving patient samples have been approved by the local Ethical Committee of Tianjin Third Central Hospital (SZX-IRB2020-005-02, Tianjin, China). Written informed consent was obtained from each patient according to the policies of the committee. The study methodologies were conformed to the standards set by the Declaration of Helsinki. All animals received humane care and complied with the approval for the use of laboratory animals by the Tianjin Medical University Animal Care and Use Committee (TMUaMEC2018025).

### Consent for publication

Not applicable.

### Competing interests

The authors declare that they have no competing interests.



**Author details**

<sup>1</sup>Department of Histology and Embryology, School of Basic Medical Sciences, Tianjin Medical University, Tianjin 300070, China. <sup>2</sup>Department of Hepatology and Gastroenterology, Tianjin Union Medical Center, Tianjin Medical University, Tianjin Union Medical Center affiliated to Nankai University, Tianjin 300000, China.

Received: 9 May 2023 Accepted: 10 November 2023

Published online: 25 November 2023

**References**

- Berumen J, Baglieri J, Kisseleva T, Mekeel K. Liver fibrosis: pathophysiology and clinical implications. *WIREs Mech Dis*. 2021;13(1):e1499.
- Bai YM, Yang F, Luo P, Xie LL, Chen JH, Guan YD, et al. Single-cell transcriptomic dissection of the cellular and molecular events underlying the triclosan-induced liver fibrosis in mice. *Mil Med Res*. 2023;10(1):7.
- Sun R, Tian X, Li Y, Zhao Y, Wang Z, Hu Y, et al. The m6A reader YTHDF3-mediated PRDX3 translation alleviates liver fibrosis. *Redox Biol*. 2022;54:102378.
- Jepsen P, Younossi ZM. The global burden of cirrhosis: a review of disability-adjusted life-years lost and unmet needs. *J Hepatol*. 2021;75(Suppl 1):S3–13.
- Weis WI, Kobilka BK. The molecular basis of G protein-coupled receptor activation. *Annu Rev Biochem*. 2018;87:897–919.
- Hauser AS, Attwood MM, Rask-Andersen M, Schiöth HB, Gloriam DE. Trends in GPCR drug discovery: new agents, targets and indications. *Nat Rev Drug Discov*. 2017;16(12):829–42.
- Baeck C, Wei X, Bartneck M, Fech V, Heymann F, Gassler N, et al. Pharmacological inhibition of the chemokine C-C motif chemokine ligand 2 (monocyte chemoattractant protein 1) accelerates liver fibrosis regression by suppressing Ly-6C<sup>+</sup> macrophage infiltration in mice. *Hepatology*. 2014;59(3):1060–72.
- Choi JW, Lee SY, Choi Y. Identification of a putative G protein-coupled receptor induced during activation-induced apoptosis of T cells. *Cell Immunol*. 1996;168(1):78–84.
- Sisignano M, Fischer MJM, Geisslinger G. Proton-sensing GPCRs in health and disease. *Cells*. 2021;10(8):2050.
- Li Z, Dong L, Dean E, Yang LV. Acidosis decreases c-Myc oncogene expression in human lymphoma cells: a role for the proton-sensing G protein-coupled receptor TDAG8. *Int J Mol Sci*. 2013;14(10):20236–55.
- Mogi C, Tobo M, Tomura H, Murata N, He XD, Sato K, et al. Involvement of proton-sensing TDAG8 in extracellular acidification-induced inhibition of proinflammatory cytokine production in peritoneal macrophages. *J Immunol*. 2009;182(5):3243–51.
- Kottyan LC, Collier AR, Cao KH, Niese KA, Hedgebeth M, Radu CG, et al. Eosinophil viability is increased by acidic pH in a cAMP- and GPR65-dependent manner. *Blood*. 2009;114(13):2774–82.
- Ihara Y, Kihara Y, Hamano F, Yanagida K, Morishita Y, Kunita A, et al. The G protein-coupled receptor T-cell death-associated gene 8 (TDAG8) facilitates tumor development by serving as an extracellular pH sensor. *Proc Natl Acad Sci U S A*. 2010;107(40):17309–14.
- Vollmer LL, Ghosal S, McGuire JL, Ahlbrand RL, Li KY, Santin JM, et al. Microglial acid sensing regulates carbon dioxide-evoked fear. *Biol Psychiatry*. 2016;80(7):541–51.
- Rackow AR, Nagel DJ, Zapas G, Clough RS, Sime PJ, Kottmann RM. The novel small molecule BTB inhibits pro-fibrotic fibroblast behavior through inhibition of rhoa activity. *Int J Mol Sci*. 2022;23(19):11946.
- Krenkel O, Tacke F. Liver macrophages in tissue homeostasis and disease. *Nat Rev Immunol*. 2017;17(5):306–21.
- Zhang K, Shi Z, Zhang M, Dong X, Zheng L, Li G, et al. Silencing lncRNA lfar1 alleviates the classical activation and pyroptosis of macrophage in hepatic fibrosis. *Cell Death Dis*. 2020;11(2):132.
- Chen T, Shi Z, Zhao Y, Meng X, Zhao S, Zheng L, et al. lncRNA Airn maintains LSEC differentiation to alleviate liver fibrosis via the KLF2-eNOS-sGC pathway. *BMC Med*. 2022;20(1):335.
- Zhang K, Han X, Zhang Z, Zheng L, Hu Z, Yao Q, et al. The liver-enriched lnc-LFAR1 promotes liver fibrosis by activating TGF $\beta$  and Notch pathways. *Nat Commun*. 2017;8(1):144.
- Zhang K, Zhang M, Yao Q, Han X, Zhao Y, Zheng L, et al. The hepatocyte-specifically expressed lnc-HSER alleviates hepatic fibrosis by inhibiting hepatocyte apoptosis and epithelial-mesenchymal transition. *Theranostics*. 2019;9(25):7566–82.
- Zhang K, Han Y, Hu Z, Zhang Z, Shao S, Yao Q, et al. SCARNA10, a nuclear-retained long non-coding RNA, promotes liver fibrosis and serves as a potential biomarker. *Theranostics*. 2019;9(12):3622–38.
- Han J, Zhang X, Lau JK, Fu K, Lau HC, Xu W, et al. Bone marrow-derived macrophage contributes to fibrosing steatohepatitis through activating hepatic stellate cells. *J Pathol*. 2019;248(4):488–500.
- Huang XP, Karpiak J, Kroeze WK, Zhu H, Chen X, Moy SS, et al. Allosteric ligands for the pharmacologically dark receptors GPR68 and GPR65. *Nature*. 2015;527(7579):477–83.
- Kimura T, Pydi SP, Wang L, Haspula D, Cui Y, Lu H, et al. Adipocyte G $\alpha_q$  signaling is a regulator of glucose and lipid homeostasis in mice. *Nat Commun*. 2022;13(1):1652.
- Sun D, Yang X, Wu B, Zhang XJ, Li H, She ZG. Therapeutic potential of G protein-coupled receptors against nonalcoholic steatohepatitis. *Hepatology*. 2021;74(5):2831–8.
- Lee JW, Lee CS, Ryu YR, Lee J, Son H, Cho HJ, et al. Lysophosphatidic acid receptor 4 is transiently expressed during cardiac differentiation and critical for repair of the damaged heart. *Mol Ther*. 2021;29(3):1151–63.
- Campbell AP, Smrcka AV. Targeting G protein-coupled receptor signalling by blocking G proteins. *Nat Rev Drug Discov*. 2018;17(11):789–803.
- Gurevich VV, Gurevich EV. Molecular mechanisms of GPCR signaling: a structural perspective. *Int J Mol Sci*. 2017;18(12):2519.
- Ghosh E, Kumari P, Jaiman D, Shukla AK. Methodological advances: the unsung heroes of the GPCR structural revolution. *Nat Rev Mol Cell Biol*. 2015;16(2):69–81.
- Xie M, Chia RH, Li D, Teo FX, Krueger C, Sabapathy K. Functional interaction between macrophages and hepatocytes dictate the outcome of liver fibrosis. *Life Sci Alliance*. 2021;4(4):e202000803.
- Nie YJ, Wu SH, Xuan YH, Yan G. Role of IL-17 family cytokines in the progression of IPF from inflammation to fibrosis. *Mil Med Res*. 2022;9(1):21.
- Justus CR, Dong L, Yang LV. Acidic tumor microenvironment and pH-sensing G protein-coupled receptors. *Front Physiol*. 2013;4:354.
- Erra Diaz F, Ochoa V, Merlotti A, Dantas E, Mazzitelli I, Gonzalez Polo V, et al. Extracellular acidosis and mTOR inhibition drive the differentiation of human monocyte-derived dendritic cells. *Cell Rep*. 2020;31(5):107613.
- Kraut JA, Madias NE. Treatment of acute metabolic acidosis: a pathophysiologic approach. *Nat Rev Nephrol*. 2012;8(10):589–601.
- Tcymbarevich I, Richards SM, Russo G, Kuhn-Georgijevic J, Cosin-Roger J, Baebler K, et al. Lack of the pH-sensing receptor TDAG8 [GPR65] in macrophages plays a detrimental role in murine models of inflammatory bowel disease. *J Crohns Colitis*. 2019;13(2):245–58.
- Gaublomme JT, Yosef N, Lee Y, Gertner RS, Yang LV, Wu C, et al. Single-cell genomics unveils critical regulators of Th17 cell pathogenicity. *Cell*. 2015;163(6):1400–12.
- Lassen KG, McKenzie CI, Mari M, Murano T, Begun J, Baxt LA, et al. Genetic coding variant in GPR65 alters lysosomal pH and links lysosomal dysfunction with colitis risk. *Immunity*. 2016;44(6):1392–405.

Ready to submit your research? Choose BMC and benefit from:

- fast, convenient online submission
- thorough peer review by experienced researchers in your field
- rapid publication on acceptance
- support for research data, including large and complex data types
- gold Open Access which fosters wider collaboration and increased citations
- maximum visibility for your research: over 100M website views per year

At BMC, research is always in progress.

Learn more [biomedcentral.com/submissions](https://biomedcentral.com/submissions)

